

1
2 **Supplementary Information for**

3
4 **Plasma membrane depolarization reveals endosomal escape incapacity of cell-**
5 **penetrating peptides**

6
7 Marc Serulla¹, Palapuravan Anees^{2,3}, Ali Hallaj¹, Evgeniya Trofimenko¹, Tara Kalia²,
8 Yamuna Krishnan^{2,3}, and Christian Widmann^{1*}

9
10 ¹Department of biomedical sciences, University of Lausanne, 1005 Lausanne,
11 Switzerland

12 ²Department of Chemistry, The University of Chicago, Chicago, Illinois 60637, USA.

13 ³Grossman Institute of Neuroscience, Quantitative Biology and Human Behavior, The
14 University of Chicago, Chicago, Illinois 60637, USA.

15 This pdf includes: materials and methods, supplementary tables and supplementary
16 figures.

Materials and methods

Chemicals

HEPES was from Sigma-Aldrich (#H4034). MES was from Carl-Roth (#4256.4), 0.05% Trypsin-EDTA was from Gibco (#25300-054). PBS was from Laboratorium Dr. Bichsel (#1000324). Propidium iodide (Sigma-Aldrich, #81845 or #P4170) was aliquoted (400 µg/ml) in water and kept at -20°C. NaCl was from Flasher Chemical (#7647-14-5), Tris from Carl Roth (#4855.1), KCl was from Fluka (#60130), NaHCO₃ and Na₂HPO₄ were from Sigma-Aldrich (#S5761 and #S7907, respectively). LLOME (L-Leucyl-L-Leucine methyl ester hydrobromide) (Sigma-Aldrich, #16689-14-8) was dissolved in water to a stock concentration of 0.7 M and kept at -20°C. Heparin sodium salt (Sigma-Aldrich, #H3149) and 2-deoxy-D-glucose (Sigma-Aldrich, #D8375) were dissolved in PBS and ddH₂O to 10 mg/ml and 1 M final concentration respectively, filtered through 0.22 µm filter (Cobetter, #SFM25PE00225), and kept at 4°C. NaN₃ (Sigma-Aldrich, # 199931) was dissolved in water and gramicidin (Sigma-Aldrich, #G5002) was dissolved in DMSO. Dextran doubly labelled with TMR and fluorescein and lysosensor DND-189 were from Thermo Fisher (#D1951 and #L7535, respectively). Bafilomycin A1 (Selleckchem, #S1413) was dissolved in DMSO to a stock concentration of 200 µM. Monensin (Sigma-Aldrich, #M5273) was dissolved in DMSO to a stock concentration of 2 mM.

Peptides

Peptides were synthesized with D-amino acids or L-amino acids as indicated in Table S9. TAMRA or Tide-Fluor 2 WS (TF2WS) were added at the indicated positions using aminocaproic acid as a linker indicated as AHX or lysine indicated as K. All peptides were synthesized by SBS Genetech CO, LTD, Beijing, China with the exception of R9-TF2WS that was from SB-PEPTIDE, Lyon France.

Cell culture and culture media

HeLa and DLD-1 cells were cultured in RPMI 1640 (#61870, Invitrogen) in 5% CO₂, 37°C incubators. For experimental purposes, we used an RPMI 1640 media from Biowest (#A0599-500) that we called “experimental medium” and that contains no sodium and no potassium (see Table S1). This medium was then supplemented with 5.3 or 100 mM KCl (Table S1), generating the so-called “control medium” and “depolarization medium”, respectively. To maintain isotonicity, NaCl was also added so that the sum of KCl and

NaCl equaled 108.77 mM (Table S1). Additionally, 5.6 mM of Na_2HPO_4 and 23.8 mM of NaHCO_3 were added to account for the inorganic salts present in RPMI 1640 (Invitrogen, #61870) (Table S1). ATP depletion was done in RPMI 1640 without glucose (Invitrogen, #11879) (Table S1). The media used in this manuscript were supplemented with 10% heat-inactivated fetal bovine serum (FBS) (#10270-106 FBS, Invitrogen).

CPP washing protocol

Cationic CPPs can interact with the cell surface largely via electrostatic interactions with proteoglycan-anchored, negatively charged glycosaminoglycans (GAGs), such as heparin sulfate and chondroitin sulfate [1-4]. Additionally, cationic CPPs strongly adhere to glass and plastic [5]. CPPs stuck on the cell surface and dish surface may be taken up by cells over time and this can misguide the analysis of CPP internalization. A triple PBS wash was insufficient to remove R9-TAMRA from the cell surface (Figure S1A, arrows and enlarged cell in the left inset) or from the dish (background signal, Figure S1A). Washing the cells with heparin cleared R9-TAMRA from the plasma membrane (Figure S1A, enlarged cell in the right inset) but had little or no effect on the R9-TAMRA background signal (Figure S1A). Trypsinizing the cells and reseeding them after the washing steps greatly reduced the background as well as cell-surface R9-TAMRA signal due to the proteolysis of the proteoglycans that carry GAGs [6, 7] (Figure S1B). The use of heparin did not further reduce the background obtained by trypsinization and reseeding (Figure S1B). Unless otherwise mentioned, the above described washing procedure was used in all experiments.

Plasma membrane potential measurement

100 mM KCl-induced plasma membrane depolarization (Figure S2A and S11B): One hundred thousand HeLa or DLD-1 cells per condition were incubated in suspension in non-adherent 24-well plates (Sarstedt, #83.3922.500) in 1 ml of regular RPMI 1640 medium, in control medium, or in depolarization medium for 30 minutes (see “Cell culture and culture media” section for the composition of these media). Plasma membrane potential was determined by incubating cells for 40 minutes with 200 nM of the DiBAC4(3) membrane potential fluorescent sensor (Thermofisher, #B438). Cells were then collected in Eppendorf tubes and cell-associated fluorescence intensity was assessed by flow cytometry. In parallel, a standard curve was generated by adding 4 $\mu\text{g}/\text{ml}$ gramicidin 30 minutes prior to DiBAC4(3) addition. DiBAC4(3) concentrations used in the standard curve

85 ranged from 0 to 1600 nM. Calculation of the actual membrane potential in mV based on
86 the DiBAC4(3) flow cytometry values was performed as described earlier [8, 9].

87 ATP depletion-induced plasma membrane depolarization (Figure S24): One hundred
88 thousand HeLa cells per condition were incubated in suspension in non-adherent 24-well
89 plates (Sarstedt, #83.3922.500) in 1 ml of regular RPMI 1640 medium or RPMI 1640
90 without glucose and supplemented with 10 mM of NaN₃ and 6 mM of 2-deoxy-D-glucose
91 for 20 minutes. Plasma membrane potential was determined as described in the previous
92 paragraph with the exception that, for the standard curve, cells were incubated with 2
93 µg/ml gramicidin for 20 minutes.

94 **Colony formation assay**

95 Fifty HeLa cells per condition were seeded overnight in 2 ml of regular RPMI 1640 medium
96 in 6-well plates (Costar, #3516). The next day, cells were washed once with 1 ml PBS and
97 cultured 2 hours in 1 ml with regular RPMI 1640 medium or RPMI 1640 containing 5.3 or
98 100 mM KCl (see Table S1). Then, cells were washed with 1 ml of PBS and cultured for
99 12 days in 2 ml of regular RPMI 1640 medium. Finally, the colonies were Giemsa stained
100 and counted.

101 **Plasma membrane permeabilization assay**

102
103 Culture media-induced toxicity (Figure S2 B left panel): One hundred thousand HeLa cells
104 per condition were seeded overnight in 12-well plates (Costar, #3513). The following day,
105 cells were washed once with PBS and incubated 2 hours in 1 ml of regular RPMI 1640
106 medium or experimental RPMI 1640 containing 5.3 or 100 mM KCl.

107
108 LLOME-induced toxicity (Figure S7C): One hundred thousand HeLa cells per condition
109 were seeded overnight in 12-well plates (Costar, #3513). The next day, cells were washed
110 once with PBS and incubated 40 minutes with experimental RPMI 1640 containing
111 100 mM KCl, PBS-washed and switched to regular RPMI 1640 medium. After 20 minutes,
112 the indicated concentrations of LLOME were added for 4 hours. Then, cells were PBS-
113 washed and cultured in RPMI 1640 medium. In both cases, 20 hours later, the media were
114 collected and kept aside, the cells were then washed with 1 ml of PBS, incubated with
115 300 µl of trypsin for 5 minutes at 37°C, collected with the media kept aside and centrifuged
116 for 3 minutes at 192 g at 4°C. Pelleted cells were resuspended in 100 µl of propidium
117 iodide (PI; 8 µg/ml) in PBS and incubated 5 minutes on ice in the dark. Finally, 300 µl of
118 PBS were added and samples were analyzed by flow cytometry.

Flow cytometry

Flow cytometry was performed with a Cytoflex S (Beckman Coulter) apparatus. Data analysis was done with the Cytexpert software (Beckman Coulter).

Calcium phosphate transient transfection

Calcium phosphate-based transfection of HeLa cells was performed as previously described [10].

Plasmids

GFP-hEEA1 (#970) and hLAMP1-GFP.dn3 (#971) encoding GFP-labeled version of human EEA1 and LAMP1, respectively, were from Addgene (#42307 and #34831). Plasmids mRFP-Rab5 and mRFP-Rab7 were received as a gift from Ari Helenius (Addgene plasmid #14437 and #14436, respectively).

Cell exposure to CPPs, washing, trypsinization and reseeding

Three hundred thousand (unless otherwise mentioned) HeLa or DLD-1 cells were seeded per well in 6-well plates (Costar, #3516) in 2 ml of regular RPMI 1640 medium and cultured overnight. The following day, cells were washed with 1 ml PBS and cultured 30 minutes in experimental RPMI 1640 containing 5.3 or 100 mM KCl. In the meantime, 35 mm glass bottom dishes (MatTek Corporation, #P35G-1.5-4-C) were coated 10 minutes with 1 mg/ml rat tail collagen (Roche, #11179179001) dissolved in 0.2% acetic acid. Unbound collagen was washed with double-distilled water. Indicated concentrations of TAMRA-labelled CPP in water were added for 10 minutes. Cells were washed three times with 1 ml PBS or once with 1 ml heparin in PBS (10 mg/ml) followed by two PBS washes as indicated in the figures and their legends. Cells were then incubated with 300 µl of trypsin for 5 minutes, collected in 1 ml regular RPMI 1640 medium and centrifuged at 192 *g* for 3 minutes, washed once more with PBS, collected again with 1 ml of regular RPMI 1640 medium, and seeded in 35 mm glass bottom collagen-coated dishes for one hour to allow cell adherence. Hoechst 33342 (1.6 µM) was added during the last 10 minutes of the indicated treatments and then the medium was replaced with 1 ml of, unless otherwise mentioned, fresh regular RPMI 1640 medium supplemented with 10 mM HEPES pre-warmed to room temperature. The cells were then imaged by confocal microscopy.

Endosomal escape detection limit

To calculate the proportion of CPPs in endosomes that would allow the detection of endosomal escape, we used various extracellular concentrations of CPPs to load endosomes. Then, we measured the initial signal in the cytosol after washing and trypsinization (Figure S25A-B). If the cytosolic signal increases by one standard deviation, we assume it can be detected (blue area in Figure S25C). The signal from the cytosol post-LLOME treatment was considered as the maximal release of endosomal content into the cytosol (mean value indicated in green in Figure S25C). The ratio of one standard deviation and the cytosolic value post-LLOME treatment represents the extent of endosomal release required for its detection (%R in Figure S25C). When cells are incubated with very low CPP concentrations (0.25 μ M), almost all the endosome-associated signal needs to be released to detect endosomal escape (Figure S25D). With increasing concentrations of CPP (≥ 2 μ M), the fraction released to detect endosomal escape decreases to values $\leq 5\%$ (Figure S25D).

Sample preparation for live confocal imaging (without the reseeding step)

For assessing CPP endosomal escape capacity just after loading the cells with the peptides, three hundred thousand HeLa cells were seeded in 35 mm glass bottom dishes (MatTek Corporation, #P35G-1.5-4-C) overnight in 2 ml of regular RPMI 1640 medium. The following day, cells were washed with 1 ml PBS and cultured 30 minutes in RPMI 1640 containing 5.33 or 100 mM KCl. Indicated concentrations of TAMRA-labelled CPP in water and Hoechst 33342 (1.6 μ M) were added for ten minutes. Cells were washed once with 1 ml of 10 mg/ml heparin in PBS followed by two PBS washes, and finally addition of fresh regular RPMI 1640 medium supplemented with 10 mM HEPES pre-warmed to room temperature. The cells were then imaged by confocal microscopy.

CPP colocalization with endosomal markers

For assessing colocalization between R9-TAMRA and endocytic markers (EEA1 and LAMP1) (Figure 1A), 100'000 Hela cells were seeded in 35 mm glass bottom dishes (MatTek Corporation, #P35G-1.5-4-C) overnight in 2 ml of regular RPMI 1640 medium. The next morning, cells were switched to DMEM supplemented with 10% FBS (Invitrogen, #10566016) and plasmid transfection was performed as indicated in the calcium transfection section of the methods. Forty-eight hours later, the medium was replaced with experimental RPMI 1640 containing 5.3 or 100 mM KCl for 30 minutes and incubated with

2 μ M of R9-TAMRA for 10 minutes. Cells were PBS-washed three times, and the addition of 1 ml fresh regular RPMI 1640 culture medium supplemented with 10 mM HEPES pre-warmed to room temperature. The cells were then imaged by confocal microscopy. Cells expressing EEA1 were imaged immediately while cells expressing LAMP1 were imaged after a 30 minute incubation period at 37°C. Percentage of colocalization was calculated visually as previously described in [11].

Colocalization of *ds-Atto₆₄₇* with endocytic tracers

To determine the trafficking time of the Voltair^{IM} through early and late endosomes and lysosomes in HeLa cells, time-dependent colocalization experiments were performed with different endocytic markers (see Figure S5). Early endosomes and late endosomes were labelled by transiently transfecting HeLa cells with plasmids encoding either Rab5-RFP or Rab7-RFP. Transfection of 150 ng of these plasmids was performed on cells grown in coverslip-containing 35 mm dish using the LipofectamineTM 2000 reagent system (Invitrogen Corporation, USA), following the manufacturer's instructions. Twenty-four hours later, the transfected cells were incubated in DMEM (Gibco, #11960-044) containing *ds-Atto₆₄₇* (500 nM) for 15 minutes, then PBS-washed three times and chased for 30 minutes, 1, 2, or 3 hours in 10% FBS-containing DMEM medium and imaged in HBSS buffer as described [12].

Endosomal membrane potential measurements

HeLa (CCL2) cells were plated at a confluency of 60-70% in 2 ml of 10% FBS-containing DMEM medium. Cells were first incubated in 1 ml of RPMI containing 5.33 or 100 mM KCl and they were then pulsed with 500 nM Voltair for 15 minutes followed by 30 minutes or 90 minutes chase periods in 1 ml RPMI containing 5.33 or 100 mM KCl as indicated in the figure legends (see Figure 1B). Images were acquired in the same chase media. Imaging was carried out on wide field microscope. After acquisition of the G (RVF channel) and R (Atto647N) images, the intracellular membrane potential was neutralized (~ 0 mV) by adding 50 μ M valinomycin and monensin in 100 mM KCl buffer for 20 minutes at room temperature (refer to the "wide-field microscopy" section for the specification of the G and R channels). Image analysis was carried out with Fiji (NIH, USA) as described in the "image analysis and quantitation" section.

Endosomal pH measurement using dextran doubly labelled with TMR and fluorescein

Fluorescein is a pH-sensitive dye while the fluorescence of TMR is not affected by pH changes. The TMR/fluorescein signal ratio can thus be used to estimate the pH of a solution. When the two dyes are coupled to cargos that are endocytosed (e.g. dextrans), it is possible to measure the pH of endosomes. Three hundred thousand HeLa cells were seeded in 35 mm glass bottom dishes (MatTek Corporation, #P35G-1.5-4-C) in 2 ml of regular RPMI medium and incubated overnight. A standard curve allowing the conversion of the TMR/fluorescein signal ratio to actual pH values was generated as described in [13] (Figure S4A). Briefly, 300'000 HeLa cells were PBS-washed, and incubated 30 minutes in regular RPMI medium with 200 µg/ml TMR- and fluorescein-doubly labelled dextran. Cells were washed 4 times with 1 ml PBS, then with 1 ml of a pH 7.5 solution and finally incubated with 1 ml of the pH 7.5 solution for 2 minutes and the signal intensity of TMR and fluorescein in endosomes determined using a confocal microscope. This procedure was incrementally repeated with the remaining pH solutions (using the most acidic solutions last) in the same cells (at least 5 images per condition). A concentration of 1.3 µM phenol red (Sigma-Aldrich, #P3532) was added to the standard curve solutions to mimic the situation found in culture media. The standard curve was used to convert the TMR/fluorescein signal ratios measured in Figure S4B to actual pH values. To assess the pH of endosomes containing dextran labelled with both TMR and fluorescein dyes (Figure S4A-B), regions of interest (ROIs) were set to encompass individual TMR labeled endosomes. Those ROIs were generated by automated thresholding ("RenyiEntropy dark"). The fluorescence intensities of each ROI were then measured in the TMR and in the fluorescein channels. This process was automated using the ImageJ-macro "spotMeasures" [14]). The TMR/fluorescein ratios were converted into pH values using the following equation that fitted the standard curve shown in Figure S4A:

$$x = \frac{\ln(10^{9.7} \cdot \frac{4.1}{y})}{1.8 \cdot \ln 10}$$

The frequency of endosomes with given pH values were then plotted (Figure S4B). Samples were treated as indicated in the legend to Figure S4B.

Endosomal pH measurement using the LysoSensor Green DND-189 pH sensor

Three hundred thousand HeLa cells were seeded in 35 mm glass bottom dishes (MatTek Corporation, #P35G-1.5-4-C) overnight in 2 ml of regular RPMI 1640 medium. The

following day, cells were washed with 1 ml PBS and cultured 30 minutes or 60 minutes in experimental RPMI 1640 containing 5.3 mM KCl or 100 mM KCl in the presence or in the absence of 200 nM Bafilomycin A1. Then, cells were exposed to 1 μ M Lysosensor green-189 for 15 minutes, washed thrice with PBS and put back in the previous media. Lysosensor green DND-189 signal quantitation was performed with ImageJ on confocal images. ROIs were drawn around lysosomes, their intensity recorded and normalized to the area of the ROIs.

ATP depletion

For imaging R9-TAMRA uptake after ATP depletion, three hundred thousand HeLa cells were seeded in 35 mm glass bottom dishes (MatTek Corporation, #P35G-1.5-4-C) overnight in 2 ml of regular RPMI 1640 medium. The following day, cells were washed with 1 ml PBS and cultured 30 minutes in regular RPMI 1640 medium or in RPMI 1640 medium lacking glucose but containing 10 mM NaN₃ and 6 mM 2-deoxy-D-glucose. The cells were then incubated with the indicated concentrations of R9-TAMRA and Hoechst 33342 (1.6 μ M) for 10 minutes. Cells were washed once with 1 ml of 10 mg/ml heparin in PBS followed by two PBS washes, and then fresh regular RPMI 1640 culture media or RPMI 1640 without glucose containing 10 mM NaN₃ and 6 mM 2-deoxy-D-glucose was added. The cells were then imaged by confocal microscopy.

Confocal microscopy

Except for Figures S5, S21, and S22, confocal imaging was performed using an LSM710 confocal microscope equipped with a Plan-Apochromat 63x/1.40 oil immersion objective (Zeiss, Oberkochen, Germany). Excitation light came from a diode (405 nm), argon laser (488 nm) and a diode-pumped solid state laser (561 nm). Live cell imaging was done using an incubation chamber set at 37°C. For time course experiments, we selected 5 fixed XY positions so that the same cells were imaged over time.

The confocal images shown in Figure S5 were captured with a Leica TCS SP5 II STED laser scanning confocal microscope (Leica Microsystems, Buffalo Grove, IL, USA) equipped with a 63x/1.4 NA, oil immersion objective. RVF and CFP were excited using an argon laser with wavelengths of 514 nm and 458 nm, respectively, and Atto647N was excited using a He-Ne laser with a wavelength of 633 nm. The Cell Mask orange stain was excited at a wavelength of 543 nm, and all emissions were filtered using an acousto-

optical beam splitter (AOBS) with settings suitable for each fluorophore and recorded using hybrid detectors (HyD).

The confocal images shown in Figure S7B were captured using a Leica Stellaris 8 confocal microscope equipped with a Plan-Apochromat 63x/1.40 oil immersion objective (Leica Microsystems, Buffalo Grove, IL, USA). Excitation light came from 405 nm and 488 diodes.

The confocal images shown in Figure S21 and S22 were captured as indicated for Figure S7B, except that the excitation light came from a diode (405 nm) and a diode-pumped solid-state laser (561 nm). Live cell imaging was done using an incubation chamber set at 37°C. For time course experiments, we selected 5 fixed XY positions so that the same cells were imaged over time. However, addition of LLOME forced the sample movement and thus the positions were not preserved after the addition of LLOME.

Wide-field microscopy

Wide-field microscopy was carried out on an IX83 inverted microscope (Olympus Corporation of the Americas, Center Valley, PA, USA) using either a 100x or 60x, 1.4 numerical aperture (NA), differential interference contrast (DIC) oil immersion objectives (PLAPON) and Evolve Delta 512 EMCCD camera (Photometrics, USA), and controlled using MetaMorph Premier Ver 7.8.12.0 (Molecular Devices, LLC, USA). Images were acquired with an exposure of 100 ms and EM gain of 100 for Atto647N, and an exposure of 200 ms and EM gain of 300 for RVF. RVF channel images were obtained using a 500/20 band-pass excitation filter, 535/30 band-pass emission filter and 89016 dichroic. For Atto647N, images were obtained using a 640/30 band-pass excitation filter, 705/72 band-pass emission filter and 89016 dichroic.

Intracellular membrane potential measurements were performed by recording images in the sensing channel (G) (i.e. the RVF channel) and normalizing channel (R) (i.e. the Atto₆₄₇ channel) in cells where each specific compartment was labelled. After acquisition of the G and R images, the intracellular membrane potential was neutralized (~ 0 mV) by adding 50 µM valinomycin and monensin in high K⁺ buffer for 20 minutes at room temperature. A set of G and R images of the same cells were acquired after valinomycin and monensin treatment. These images of neutralized endosomes were used as a baseline measurement to correct for variations in autofluorescence. To record all endosomal compartments in the cell, Z-stacks (20 planes, Z distance = 0.8 µm) were captured and a maximum intensity projection was used to produce a single image for analysis.

Image analysis and quantitation

All images were quantitated using the ImageJ (Fiji) software [15] except images from Figure 1B that were quantified visually as described in [16].

To assess the amount of CPP cytosolic staining we used two methods (schematically described in Figure S26A): *i*) manual quantitation based on the analysis of circular region of interest (ROI) drawn within the nucleus or in the cytosol in regions lacking endosomes; *ii*) quantitation based on automated selection of ROI. For nuclear automated quantitation, a mask corresponding to the Hoechst staining was used as an ROI. For cytosolic quantitation, a mask was created based on Hoechst staining, this mask was duplicated and extended by 1 μm . The area of the first mask was removed from the extended mask, creating a perinuclear cytosolic ring. For both the nuclear and cytosolic quantitation, signal corresponding to endosomal R9-TAMRA was removed from the ROI (Figure S26B) by an automated ("YEN dark") threshold approach (the codes for the automated quantitation are deposited here [<https://github.com/marcseru/Fiji-diffuse-staining-analysis.git>]). Automated analysis was working adequately only when the endosomal signal was predominant over the cytosolic signal (Figure S27). Thus, images with predominant diffuse staining (i.e. cytosolic) were analyzed using manual quantitation. The chosen way of image analysis (automated or manual) is indicated in the figure legends. Background values were obtained by drawing a circular ROI in five different areas without cells per image (Figure S27).

To assess the number of endosomes per cell (Figure S3), we used a previously described protocol [17]. Briefly, we reanalyzed images from Figure 1A treated with 1 μM R9-TAMRA. The parameters used to identify endosomes in the images were the following: particle size (0.25-4 μm^2), spot circularity (0.1-1), sigma radius (3), filtering method (DoG), auto-threshold (triangle). The ROI was manually defined as the whole image area. To get the endosomes per cell ratio in each image the total number of identified spots were divided by the number of nuclei (nuclei that were only partially located in the image were not considered).

For single-cell time course analyses, the cytosolic fluorescence (Figure S8) was recorded from Figure S6 images (condition without LLOME). An ROI was manually placed in the cytosol of the cells and fluorescence intensity was measured.

To quantitate colocalization between endocytic markers and ds-Atto₆₄₇ (Figure S5), we used Pearson's correlation coefficients that measure the pixel-by-pixel covariance of two

images. Pearson's correlation coefficients range from 0 to 1, 1 indicating complete colocalization. These coefficients were calculated using ImageJ/Fiji 2.0.0-rc-54/1.51 h. For endosome voltage measurements (Figure 1B), regions of cells containing single isolated endosomes in each Atto₆₄₇N (R) image were manually selected and the coordinates of the region outside the endosomes were manually selected and saved as ROIs. The same regions were selected in the RVF (G) image by recalling the ROIs. After background subtraction, the mean intensity for each endosome (G and R signals) was measured and exported to OriginPro (OriginLab, USA). A ratio of G to R intensities (G/R) was obtained from these values by dividing the mean intensity of a given endosome in the G image with the corresponding intensity in the R image. To minimize the measurement error due to low fold change of the Voltair probes, the same endosomes within live cells were measured post addition of valinomycin and monensin, which neutralized the membrane potential in the presence of 100 mM KCl. For a given experiment, the membrane potential of an organelle population was determined as described previously [12]. The original publication describing the use of Voltair [12] presents schematically in its Extended Data Fig. 1 how endosomal membrane potential is measured.

ATP measurement

Two hundred thousand wild-type HeLa cells per condition were seeded overnight in RPMI 1640 medium in 6-well plates (Costar, #3516). Cells were PBS-washed and incubated 20 minutes with 1 ml of either RPMI 1640 without glucose containing 10 mM of NaN₃ and 6 mM of 2-deoxy-D-glucose or regular RPMI 1640 medium. Cells were PBS-washed, trypsinized with 300 µl of the trypsin/EDTA solution for 5 minutes, collected with 1 ml PBS, pelleted at 192 g for 3 minutes, PBS-washed and resuspended in 100 µl lysis buffer (20 mM Na₂CO₃ and 100 mM NaHCO₃ in water). Tubes were placed immediately at -80°C and kept at this temperature overnight. Intracellular ATP content was measured with an ATP determination kit (#A22066, Molecular Probes) according to manufacturer's instructions. Briefly, cell lysates and ATP standards (10 µl) were mixed with standard reaction solution (90 µl) and luminescence was determined using an automatized bioluminometer (Promega Glomax 96 microplate luminometer). ATP level for each sample was normalized to protein content measured by Bradford reaction.

Statistics

386 Statistical analyses were performed using GraphPad Prism version 8.0.0 for Windows,
387 GraphPad Software, San Diego, California USA, www.graphpad.com. In the figures, the
388 p values that are above 5% are shaded in grey while those below 5% are indicated in
389 black.
390

Supplementary references

1. Ghibaudi, E., et al., *The interaction of the cell-penetrating peptide penetratin with heparin, heparansulfates and phospholipid vesicles investigated by ESR spectroscopy*. J Pept Sci, 2005. **11**(7): p. 401-9.
2. Ziegler, A. and J. Seelig, *Interaction of the protein transduction domain of HIV-1 TAT with heparan sulfate: binding mechanism and thermodynamic parameters*. Biophysical journal, 2004. **86**(1 Pt 1): p. 254-263.
3. Rullo, A., J. Qian, and M. Nitz, *Peptide-glycosaminoglycan cluster formation involving cell penetrating peptides*. Biopolymers, 2011. **95**(10): p. 722-731.
4. Hakansson, S. and M. Caffrey, *Structural and dynamic properties of the hiv-1 tat transduction domain in the free and heparin-bound states*. Biochemistry, 2003. **42**(30): p. 8999-9006.
5. Chico, D.E., R.L. Given, and B.T. Miller, *Binding of cationic cell-permeable peptides to plastic and glass*. Peptides, 2003. **24**(1): p. 3-9.
6. Moody, H.R., et al., *In vitro degradation of articular cartilage: does trypsin treatment produce consistent results?* Journal of anatomy, 2006. **209**(2): p. 259-267.
7. Hoogewerf, A.J., et al., *Effect of chlorate on the sulfation of lipoprotein lipase and heparan sulfate proteoglycans. Sulfation of heparan sulfate proteoglycans affects lipoprotein lipase degradation*. Journal of Biological Chemistry, 1991. **266**(25): p. 16564-16571.
8. Krasznai, Z., et al., *Flow cytometric determination of absolute membrane potential of cells*. J Photochem Photobiol B, 1995. **28**(1): p. 93-9.
9. Klapperstuck, T., et al., *Methodological aspects of measuring absolute values of membrane potential in human cells by flow cytometry*. Cytometry A, 2009. **75**(7): p. 593-608.
10. Jordan, M., A. Schallhorn, and F.M. Wurm, *Transfecting mammalian cells: optimization of critical parameters affecting calcium-phosphate precipitate formation*. Nucleic Acids Res, 1996. **24**(4): p. 596-601.
11. Trofimenko, E., et al., *The endocytic pathway taken by cationic substances requires Rab14 but not Rab5 and Rab7*. Cell Reports, 2021. **37**(5): p. 109945.
12. Saminathan, A., et al., *A DNA-based voltmeter for organelles*. Nat Nanotechnol, 2021. **16**(1): p. 96-103.
13. Ma, L., et al., *Live-cell microscopy and fluorescence-based measurement of luminal pH in intracellular organelles*. Frontiers in Cell and Developmental Biology, 2017. **5**(71).
14. Herbie. *Quantification of fluorescence spots intensity along the spot area*. 2018 01.12.2018 [cited 2021 19.07.2021].
15. Schindelin, J., et al., *Fiji: an open-source platform for biological-image analysis*. Nature Methods, 2012. **9**(7): p. 676-682.
16. Trofimenko, E., et al., *The endocytic pathway taken by cationic substances requires Rab14 but not Rab5 and Rab7*. Cell Rep, 2021. **37**(5): p. 109945.
17. Bayle, V., M.P. Platre, and Y. Jaillais, *Automatic quantification of the number of intracellular compartments in Arabidopsis thaliana root cells*. Bio Protoc, 2017. **7**(4).

Supplementary tables

Table S1. The composition of the media used in this work. Where indicated, media were supplemented with 10% FBS as described in the method section. Components that were added to the sodium- and potassium-free RPMI 1640 medium (Biowest #A0599-500; i.e. the so-called experimental medium) to get the “control” (5.3 mM KCl) or “depolarization” (100 mM KCl) media are indicated in red. “=”, same composition as regular RPMI 1640 (Invitrogen, #61870); “/”, component not present in the medium.

	(mM)		
	RPMI 1640 (Invitrogen, #61870) (Regular)	RPMI 1640 (Biowest, #A0599-500) (in red, salts added to get the control or depolarizing media)	RPMI1640 (Invitrogen, #11879) (w/o glucose)
Amino acids			
Glycine	0.13	=	=
L-Alanyl-Glutamine	2.1	/	/
L-Arginine	1.1	=	=
L-Asparagine	0.38	=	=
L-Aspartic acid	0.15	=	=
L-Cystine	0.21	=	=
L-Glutamic Acid	0.14	=	=
L-Histidine	0.097	=	=
L-Hydroxyproline	0.15	=	=
L-Isoleucine	0.38	=	=
L-Leucine	0.38	=	=
L-Lysine hydrochloride	0.22	=	=
L-Methionine	0.1	=	=
L-Phenylalanine	0.091	=	=
L-Proline	0.17	=	=
L-Serine	0.29	=	=
L-Threonine	0.17	=	=
L-Tryptophan	0.025	=	=
L-Tyrosine	0.11	=	=
L-Valine	0.17	=	=
L-Glutamine	/	2.06	2.06
Vitamins			
Biotin	$8.2 \cdot 10^{-4}$	=	=
Choline chloride	0.021	=	=
D-Calcium pantothenate	$5.2 \cdot 10^{-4}$	=	=
Folic Acid	0.002	=	=
Niacinamide	0.008	=	=
Para-Aminobenzoic Acid	0.007	=	=
Pyridoxine hydrochloride	0.005	=	=

Riboflavin	$5.3 \cdot 10^{-4}$	=	=
Thiamine hydrochloride	0.003	=	=
Vitamin B12	$3.7 \cdot 10^{-6}$	=	=
i-Inositol	0.19	=	=
Inorganic salts			
Calcium nitrate ($\text{Ca}(\text{NO}_3)_2 \cdot 4\text{H}_2\text{O}$)	0.42	=	=
Magnesium Sulfate ($\text{MgSO}_4 \cdot 7\text{H}_2\text{O}$)	0.41	=	=
Potassium Chloride (KCl)	5.3	5.3 or 100	=
Sodium Bicarbonate (NaHCO_3)	23.8	23.8	=
Sodium Chloride (NaCl)	103	103 or 8.8	=
Sodium Phosphate dibasic (Na_2HPO_4) anhydrous	5.6	5.6	=
Other Components	11		
D-Glucose (Dextrose)	11	=	/
Glutathione (reduced)	0.003	=	=
Phenol Red	0.013	=	=

446
447

Table S2. P values related to Figure 2A. This table displays the p values for a given condition versus the control 0 μ M R9-TAMRA condition. Data were converted to log₁₀(x) and then two-way ANOVAs with Dunnett's post-hoc test were performed; p values above 5% are highlighted in grey.

		R9-TAMRA [μ M]				
		1	2	5	10	20
Cytosol	5.3 mM KCl	0.15	<0.001	<0.001	<0.001	<0.001
	100 mM KCl	0.993	0.004	<0.001	<0.001	<0.001
Nucleus	5.3 mM KCl	0.97	<0.001	<0.001	<0.001	<0.001
	100 mM KCl	0.999	0.5894	<0.001	<0.001	<0.001

Table S3. P values related to Figure 3A. This table displays the p values against conditions without TAT-TAMRA. Data were converted to log₁₀(x) and then two-way ANOVAs with Dunnett's post-hoc test were performed against the condition without TAT-TAMRA; p values above 5% are highlighted in grey.

		TAT-TAMRA [μ M]				
		1	2	5	10	20
Cytosol	5.3 mM KCl	0.969	<0.001	<0.001	<0.001	<0.001
	100 mM KCl	0.998	0.589	<0.001	<0.001	<0.001
Nucleus	5.3 mM KCl	0.997	<0.001	<0.001	<0.001	<0.001
	100 mM KCl	0.999	0.999	<0.001	<0.001	<0.001

Table S4. P values related to Figure S13. This table displays the p values against conditions without D-dfTAT-TAMRA. Data were converted to log₁₀(x) and then two-way ANOVAs with Dunnett's post-hoc test were performed against the condition without D-dfTAT-TAMRA.

		D-dfTAT-TAMRA [μ M]				
		1	2	5	10	20
Cytosol	5.3 mM KCl	<0.001	<0.001	<0.001	<0.001	<0.001
	100 mM KCl	<0.001	<0.001	<0.001	<0.001	<0.001
Nucleus	5.3 mM KCl	<0.001	<0.001	<0.001	<0.001	<0.001
	100 mM KCl	<0.001	<0.001	<0.001	<0.001	<0.001

Table S5. P values related to Figure S17. This table displays the p values against conditions without CPP12-TAMRA. Data were converted to log₁₀(x) and then two-way ANOVAs with Dunnett's post-hoc test were performed against the condition without CPP12-TAMRA; p values above 5% are highlighted in grey.

		CPP12-TAMRA [μ M]				
		1	2	5	10	20
Cytosol	5.3 mM KCl	0.997	0.985	<0.001	<0.001	<0.001
	100 mM KCl	>0.999	0.997	<0.001	<0.001	<0.001
Nucleus	5.3 mM KCl	0.996	0.984	<0.001	<0.001	<0.001
	100 mM KCl	>0.999	>0.999	<0.001	<0.001	<0.001

Table S6. P values related to Figure S20. This table displays the p values against conditions without ZF5.3-TAMRA. Data were converted to log₁₀(x) and then two-way ANOVAs with Dunnett's post-hoc test were performed against the condition without ZF5.3-TAMRA; p values above 5% are highlighted in grey.

		ZF5.3-TAMRA [μ M]				
		1	2	5	10	20
Cytosol	5.3 mM KCl	0.982	>0.999	<0.001	<0.001	<0.001
	100 mM KCl	0.999	0.999	0.013	<0.001	<0.001
Nucleus	5.3 mM KCl	0.933	0.972	<0.001	<0.001	<0.001
	100 mM KCl	>0.999	>0.999	0.006	<0.001	<0.001

Table S7. P values related to Figure S22. This table displays the p values against conditions without TAT-RasGAP₃₁₇₋₃₂₆-TAMRA. Data were converted to log₁₀(x) and then two-way ANOVAs with Dunnett's post-hoc test were performed against the condition without TAT-RasGAP₃₁₇₋₃₂₆-TAMRA.

		TAT-RasGAP ₃₁₇₋₃₂₆ [μM]				
		1	2	5	10	
Cytosol	5.33 mM KCl	<0.001	<0.001	<0.001	<0.001	<0.001
	100 mM KCl	<0.001	<0.001	<0.001	<0.001	<0.001

Table S8. P values related to Figure S23. This table displays the p values against conditions without OTX2(HD)-TAMRA. Data were converted to log₁₀(x) and then two-way ANOVAs with Dunnett's post-hoc test were performed against the condition without OTX2(HD)-TAMRA.

		OTX2 (HD) [μ M]				
		1	2	5	10	20
Cytosol	5.33 mM KCl	<0.001	<0.001	<0.001	<0.001	<0.001
	100 mM KCl	<0.001	<0.001	<0.001	<0.001	<0.001

Table S9. Peptides used in the present study. The initial bold N and C letters in the sequences indicate the amino- and carboxy-terminal end of the peptide, respectively. The other letters in the sequence correspond to the one letter amino acid code. AHX refers to aminocaproic acid and Φ refers to 2-Nal. Lower case letters indicate L-amino acids and upper case letters indicate D-amino acids.

Peptide name	Sequence	Enantiomer
R9-TAMRA	N -TAMRA-AHX-RRRRRRRRR- C	D
R9-TF2WS	N -TF2WS-AHX-rrrrrrrrr- C	L
TAT	N -TAMRA- AHX-RRRQRRKKRG- C	D
D-dfTAT	N -ck-TAMRA-RKKRRQRRRG- C N -ck-TAMRA-RKKRRQRRRG- C	D
CPP12	Cyclo(F Φ RrRrQ)-K-TAMRA	D and L
ZF5.3	N -k-TAMRA-wyscnvcgkafvlshrlnrvhrrat- C	L
TAT-RasGAP ₃₁₇₋₃₂₆	N -TAMRA-AHX-DTRLNTVMMWGRRRQRRKKRG- C	D
OTX2(HD)-TAMRA	N -TAMRA-AHX- QRRERTTFTRAQLDVLEALFAKTRYPDIFMR EEVALKINLPESRVQWVFNRRRAKCRQQQ- C	D

Supplementary figure legends

Figure S1. CPP washing protocol set-up. A. The experimental conditions are depicted schematically above the data. HeLa cells were cultured 30 minutes in 5.3 mM KCl RPMI 1640 control media and exposed for 10 minutes to the indicated concentrations of R9-TAMRA. Then, cells were washed either three times with PBS or one time with 10 mg/ml heparin in PBS followed by two PBS washes and cultured again in 5.3 mM KCl control medium. Fifty minutes later, Hoechst 33342 (1.6 μ M) was added for 10 minutes. The medium was then discarded and replaced with fresh RPMI 1640 medium pre-warmed at room temperature. The cells were immediately imaged by confocal microscopy. Representative images (scale bar: 20 μ m) from two independent experiments are shown. Arrows point to examples of cells with surface R9-TAMRA staining. Two cells are enlarged to show the difference between cell surface staining and no surface staining. Quantitation shown on the right corresponds to the signal detected outside cells (background signal). This was done by positioning ROIs manually so that they did not overlap with any cells (dotted circles are examples of such ROIs). Grey bar represents the median. For statistical analysis, data were transformed to $\log_{10}(x)$ prior to one-way ANOVA test analysis with Sidak's post-hoc test for the equal R9-TAMRA concentration pairs and with Dunnett's post-hoc test for the comparison without peptide. **B.** As panel A, except that cells were trypsinized and reseeded on collagen-coated glass-bottom dishes.

Figure S2. High potassium buffer triggers plasma membrane depolarization in HeLa cells. The experimental conditions are depicted schematically above the data. **A.** One hundred thousand HeLa cells per condition were incubated 30 minutes in regular RPMI 1640 medium or RPMI 1640 experimental media containing 5.3 mM or 100 mM of KCl. Membrane potential was then determined using the DiBAC4(3) sensor. **B.** HeLa cells were cultured 2 hours in the indicated culture media and cell viability was evaluated either after 22 hours later by PI staining or after 12 days by colony formation assay.

Figure S3. Plasma membrane depolarization does not affect the number of R9-TAMRA containing endosomes. Endosome number quantitation was performed on the images acquired in Figure 1A, using the 1 μ M R9-TAMRA condition that led to similar

cytosolic CPP fluorescence in control and depolarization media. Quantitation was done using an ImageJ automated process as described in the methods.

Figure S4. Plasma membrane depolarization does not affect endosomal pH. **A.** Cells were PBS-washed and switched to fresh RPMI 1640 regular medium and incubated with TMR- and fluorescein-labelled dextran (200 µg/ml) for 30 minutes. Cells were exposed to media with different pH to generate a standard curve allowing the conversion of TMR/fluorescein ratios into actual pH values (see the methods for details). The images on the right show three examples of TMR and fluorescein signals in cells exposed to different pH. **B.** The experimental conditions are depicted schematically on the left of the graph. The pH of individual endosomes was recorded in >400 endosomes from at least 5 images per condition derived from three independent experiments as described in the methods. Each dot represents an experiment. The lines go through the average values of a given condition. The images are representative examples of the endosomal staining obtained in the three tested conditions. **C.** The experimental conditions are depicted schematically above the data. The fluorescence of LysoSensor Green DND-189 increases as the pH decreases. As bafilomycin A1 was dissolved in DMSO, an equivalent volume of DMSO was added in the “no bafilomycin A1” condition. Image analysis was performed as indicated in the methods. Statistical analysis: unpaired t-tests.

Figure S5. Time dependent trafficking of *ds-Atto*₆₄₇. Representative images of colocalization in HeLa cells between *ds-Atto*₆₄₇ and the indicated RFP-labelled endosomal markers. Quantitation of these colocalization events, assessed by Pearson's correlation, is shown on the right-hand side of the images. Rab5-RFP and Rab7-RFP label early and late endosomes, respectively. The cells were transfected with plasmids encoding the Rab5 or Rab7 constructs 48 hours before *ds-Atto*₆₄₇ addition. The *ds-Atto*₆₄₇ compound was added to cells for 15 minutes and then chased for the indicated periods of time. Images were then taken using a confocal microscope. Scale bars, 10 µm. Arrows indicate the zones that were enlarged in the insets. Cell contours are indicated. The green signal corresponds to RFP-positive endosomes and the red signal correspond to *Atto*₆₄₇-positive endosomes.

Figure S6. R9 does not escape endosomes unless triggered by LLOME. The experimental conditions are depicted schematically above the data. Representative images (scale bar: 20 µm) from two independent experiments are shown. Image analysis

was automated as described in the methods except for the conditions with 0.25 mM of LLOME that was quantitated manually. Each dot represents an individual cell and black bars represent the median. For statistical analysis, data were transformed to $\log_{10}(x)$ prior to applying one-way ANOVAs with Dunnett's post-hoc test against the "60 min" condition.

Figure S7. Evaluation of LLOME toxicity and effect. A. The experimental conditions are depicted schematically above the data. Three hundred thousand HeLa cells were cultured 30 minutes with RPMI 1640 containing 100 mM of KCl and exposed for 10 minutes to 2 μ M of R9-TAMRA. Then, cells were washed, trypsinized, and seeded on collagen-coated glass-bottom dishes for confocal imaging in RPMI 1640 media. Hoechst (1.6 μ M) was added 10 minutes before imaging and then media was switched to 1 ml of regular RPMI 1640 media. Confocal images were taken before and 30 minutes after the addition of 1 ml of RPMI culture media containing 0.1, 0.25 mM, or no LLOME. Representative images (scale bar: 20 μ m). Image analysis was performed with automated analysis except for the conditions with 0.25 mM of LLOME that was quantitated manually. Each dot represents an individual cell and black bars represent the median. For statistical analysis data were transformed to $\log_{10}(x)$ prior to applying a one-way ANOVA test with Dunnett's post-hoc test between the selected pairs. **B.** The experimental conditions and data analysis are identical to those used in Figure 2B, except that R9-TF2WS was used instead of R9-TAMRA. Representative images (scale bar: 15 μ m) from three independent experiments are shown. **C.** The experimental conditions are depicted schematically at the top of the panel. At the end of the treatment, the cells were washed thrice with 1 ml PBS, trypsinized, collected, PI-stained (8 μ g/ml) and cell death analyzed by flow cytometry.

Figure S8. Single cell analysis of cytosolic fluorescence variation over time following CPP endosomal loading. Cell images from the condition without LLOME in Figure 2 were used to quantitate the cytosolic fluorescence in single cells at different time points after CPP endosomal loading. Quantitation was performed as described in the methods using the Image J software.

Figure S9. R9 does not escape from endosomes whether the cells are depolarized or not. The experimental conditions are depicted schematically above the data. Representative images (scale bar: 20 μ m) from two independent experiments are shown. Image analysis was automated as described in the methods except for the conditions with 0.25 mM of LLOME that was quantitated manually. Each dot represents an individual cell

and black bars represent the median. For statistical analysis, data were transformed to $\log_{10}(x)$ prior applying one-way ANOVAs with Dunnett's post-hoc test against the "60 min" condition.

Figure S10. Loading cells with 5 μ M R9 does not lead to CPP endosomal escape.

Same experimental conditions as in Figure 2, except that 5 μ M of R9-TAMRA were used instead of 2 μ M.

Figure S11. R9 does not escape endosomes in DLD-1 cells. A. The experimental conditions are depicted schematically at the top of the panel. Representative images (scale bar: 20 μ m) from two independent experiments are shown. Quantitation was automated as described in the methods except for the "0.5 mM LLOME" condition where quantitation was done manually. Each dot represents an individual cell and black bars correspond to the median. For statistical analysis, data were transformed to $\log_{10}(x)$ prior to applying one-way ANOVAs with Dunnett's post-hoc test against the "time 60 min" condition. **B.** Extent of depolarization induced by 100 mM KCl in DLD-1 cells. Cells were treated as in Figure 1A.

Figure S12. No evidence for R9 endosomal escape right after endosomal loading.

The experimental conditions are depicted schematically at the top of the panel. Representative images (scale bar: 20 μ m) from two independent experiments are shown. Manual analysis was done for all conditions. For statistical analyses, data were transformed to $\log_{10}(x)$ prior to applying one-way ANOVAs with Dunnett's post-hoc tests against time 0.

Figure S13. D-dfTAT uptake in control and depolarized cells. Hela cells were subjected to the experimental conditions depicted schematically at the top of the panel. Representative images (scale bar: 20 μ m) from two independent experiments are shown. Quantitation was performed with the automated procedure described in the methods except for the 5, 10, and 20 μ M of D-dfTAT-TAMRA conditions in the presence of 5.3 mM of KCl and for the 10 and 20 μ M D-dfTAT-TAMRA conditions in the presence of 100 mM of KCl that were quantitated manually. Grey bars correspond to the median. For statistical analyses of the indicated conditions, data were transformed to $\log_{10}(x)$ prior to two-way

ANOVAs followed with Sidak's post-hoc test. The comparison with the "0 μ M D-dfTAT-TAMRA" condition is presented in Table S4.

Figure S14. Endosome-associated D-dfTAT does not translocate to the cytosol. The experimental conditions are depicted schematically above the data. Representative images (scale bar: 20 μ m) from two independent experiments are shown. Image analysis was performed with automated analysis except for the conditions with 0.25 mM of LLOME that was quantitated manually. Each dot represents an individual cell and black bars correspond to the median. For statistical analysis, data were transformed to $\log_{10}(x)$ prior to applying one-way ANOVAs with Dunnett's post-hoc tests against the "time 60 min" condition.

Figure S15. D-dfTAT does not escape endosomes but can access the cytosol from the plasma membrane-associated pool. The experimental conditions are depicted schematically above the data. Representative images (scale bar: 20 μ m) from two independent experiments are shown. Image analysis was performed manually in all the conditions. For statistical analysis, data were transformed to $\log_{10}(x)$ prior to applying one-way ANOVAs with Dunnett's post-hoc test against the "time 0 min" condition. Arrows point towards cell surface staining. Note that when D-dfTAT was washed with PBS only, but not when the cells were washed with heparin, a little increase in cytosolic signal was observed overtime. This is likely occurring as a result of direct translocation of peptides that remained bound to the plasma membrane.

Figure S16. D-dfTAT does not escape endosomes in non-depolarized cells. The experimental conditions are depicted schematically above the data. Representative images (scale bar: 20 μ m) from two independent experiments are shown. Image analysis was performed manually in all cases. For statistical analysis, data were transformed to $\log_{10}(x)$ prior to applying one-way ANOVAs with Dunnett's post-hoc test against the "time 0 min" condition.

Figure S17. CPP12 uptake in control and depolarized cells. HeLa cells were subjected to the experimental conditions depicted schematically at the top of the panel. Representative images (scale bar: 20 μ m) from two independent experiments are shown. Quantitation was performed with the automated procedure described in the methods, except for the 5, 10, and 20 μ M CPP12-TAMRA conditions in the presence of 5.3 mM KCl

and for the 20 μ M CPP12-TAMRA condition in the presence of 100 mM KCl that were quantitated manually. Grey bars correspond to the median. For statistical analyses of the indicated conditions, data were transformed to $\log_{10}(x)$ prior to two-way ANOVAs followed with Sidak's post-hoc test. The comparison with the "0 μ M D-dfTAT-TAMRA" condition is presented in Table S5.

Figure S18. No evidence of CPP12 endosomal escape in non-depolarized cells. The experimental conditions are depicted schematically above the data. Representative images (scale bar: 20 μ m) from two independent experiments are shown. Image analysis was performed manually in all cases. For statistical analysis, data were transformed to $\log_{10}(x)$ prior to applying one-way ANOVAs with Dunnett's post-hoc test against the "time 0 min" condition.

Figure S19. No evidence for CPP12 endosomal escape in cells loaded with 5 μ M of the peptide. The experimental conditions are depicted schematically above the data. Representative images (scale bar: 20 μ m) from two independent experiments are shown. Image analysis was performed manually in cases. For statistical analysis data were transformed to $\log_{10}(x)$ prior applying one-way ANOVAs with Dunnett's post-hoc test against the "time 0 min" condition.

Figure S20. ZF5.3 cytosolic uptake in control and depolarized cells. Hela cells were subjected to the experimental conditions depicted schematically at the top of the panel. Representative images (scale bar: 20 μ m) from two independent experiments are shown. Quantitation was performed with the automated procedure described in the methods except for the 20 μ M ZF5.3-TAMRA condition that was quantitated manually. Grey bars correspond to the median. For statistical analyses of the indicated conditions, data were transformed to $\log_{10}(x)$ prior to two-way ANOVAs followed with Sidak's post-hoc test. The comparison with the "0 μ M ZF5.3 -TAMRA" condition is presented in Table S6.

Figure S21. ZF5.3 does no escape endosomes. The experimental conditions are depicted schematically above the data. Representative images (scale bar: 20 μ m) from two independent experiments are shown. Image analysis was performed manually in all

conditions. For statistical analysis, data were transformed to $\log_{10}(x)$ prior to applying one-way ANOVAs with Dunnett's post-hoc test against the "time 0" condition.

Figure S22. TAT-RasGAP₃₁₇₋₃₂₆ does not escape endosomes A. The experimental conditions are depicted schematically above the data. Representative images (scale bar: 20 μm) from two independent experiments are shown. Quantitation was performed with the automated procedure described in the methods except for the 10 and 20 μM TAT-RasGAP₃₁₇₋₃₂₆-TAMRA conditions in the presence of 5.3 mM and 100 mM of KCl that were quantitated manually. Grey bars represent the median. For statistical analyses of the indicated conditions, data were transformed to $\log_{10}(x)$ prior to two-way ANOVAs followed with Sidak's post-hoc test. The comparison with the "0 μM TAT-RasGAP₃₁₇₋₃₂₆-TAMRA" condition is presented in Table S7. **B.** The experimental conditions are depicted schematically above the data. Representative images (scale bar: 20 μm) from two independent experiments are shown. Quantitation was performed with the automated procedure described in the methods except for the conditions with 0.25 mM of LLOME that were manually quantitated. Each dot represents an individual cell and black bars correspond to the median. For statistical analyses, data were transformed to $\log_{10}(x)$ prior to applying one-way ANOVAs with Dunnett's post-hoc tests against the "60 min" condition

Figure S23. OTX2(HD) does not escape endosomes. A. The experimental conditions are depicted schematically above the data. Representative images (scale bar: 20 μm) from two independent experiments are shown. Quantitation was performed with the automated procedure described in the methods except for the 20 μM OTX2(HD)-TAMRA conditions in the presence of 5.3 mM and 100 mM of KCl that were quantitated manually. Grey bars represent the median. For statistical analyses of the indicated conditions, data were transformed to $\log_{10}(x)$ prior to two-way ANOVAs followed with Sidak's post-hoc test. The comparison with the "0 μM OTX2(HD)-TAMRA" condition is presented in Table S8. **B.** The experimental conditions are depicted schematically above the data. Representative images (scale bar: 20 μm) from two independent experiments are shown. Quantitation was performed with the automated procedure described in the methods except for the conditions with 0.25 mM of LLOME that were manually quantitated. Each dot represents an individual cell and black bars correspond to the median. For statistical

analyses, data were transformed to $\log_{10}(x)$ prior to applying one-way ANOVAs with Dunnett's post-hoc tests against the "60 min" condition.

Figure S24. ATP depletion blocks R9 direct translocation and endocytic uptake. A.

Two hundred thousand HeLa cells were PBS-incubated 20 minutes with 1 ml of regular RPMI 1640 or 1 ml of RPMI 1640 without glucose containing 10 mM of NaN_3 and 6 mM of 2-deoxy-D-glucose. Cells were collected and ATP level was measured as described in the methods. **B.** One hundred thousand HeLa cells per condition were incubated 30 minutes with 1 ml of regular RPMI 1640 or 1 ml of RPMI 1640 without glucose containing 10 mM of NaN_3 and 6 mM of 2-deoxy-D-glucose. Membrane potential was then determined using the DiBAC4(3) sensor. **C.** Three hundred thousand HeLa cells were cultured 30 minutes in regular RPMI 1640 or 1 ml of RPMI 1640 without glucose containing 10 mM of NaN_3 and 6 mM of 2-deoxy-D-glucose in the presence of the indicated concentrations of R9-TAMRA. Hoechst 33342 (1.6 μM) was added for the last 10 minutes. Cells were washed once with 1 ml of 10 mg/ml heparin salt in PBS followed by two PBS washes and placed in the culture media they were exposed to initially but without CPPs. The cells were then imaged by confocal microscopy.

Figure S25. CPP endosomal escape detection limit. The experimental conditions are depicted schematically above the data. Representative images (scale bar: 20 μm) from two independent experiments are shown. Image quantitation was performed manually in all conditions (left lower graph). Here we assumed that an increase of one standard deviation over the basal cytosolic signal allows detection of CPP endosomal escape. The ratio between one standard deviation and the total CPP endosomal content, determined by measuring the cytosolic signal obtained after LLOME addition, gives the minimal proportion of CPP that need to leave the endosomes to allow endosomal escape detection (right lower graph). Note that the proportion calculated for the 5 μM condition is overestimated because the LLOME signal at this concentration saturates.

Figure S26. Methodologies for the quantitation of CPP cytosolic staining. A-B.

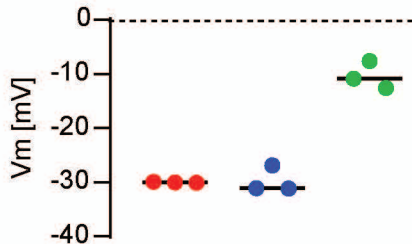
Schemes depicting the manual and automated quantitation of CPPs in the nucleus and in the cytoplasm. For clarity, the CPP fluorescence is not depicted in these schemes. It should be understood though that the shown endosomes are those that contain the CPPs. See the main text and method section for details. **C.** Representative examples of the

777 automated processes that generate the regions of interest (ROI) used to quantitate
778 cytoplasmic or nuclear CPP signal.

779 **Figure S27. Comparison between manual and automated quantitation of CPP**
780 **cytosolic staining.** The manual and automated quantitation methodologies described in
781 Figure S26 were used to analyze the data shown in Figure 1C. Results are shown as violin
782 plots. Grey bars represent the median. For statistical analysis, data were transformed to
783 $\log_{10}(x)$ before applying two-way ANOVA tests with Sidak's post-hoc test (when
784 comparing data at a given concentration) or with Dunnett's post-hoc test (when making
785 the comparison with the "0 μ M R9-TAMRA" condition). In the latter case, p values > 0.05
786 are colored in dark green.

A

- Regular culture medium (5.3 mM KCl)
- Control medium (5.3 mM KCl)
- Depolarization medium (100 mM KCl)



B

PBS wash and switch to regular RPMI culture medium

2 hours in following media:

- Regular (5.3 mM KCl)
- Control (5.3 mM KCl)
- Depolarization (100 mM KCl)

22 hours	PI staining
12 days	Colony formation assay

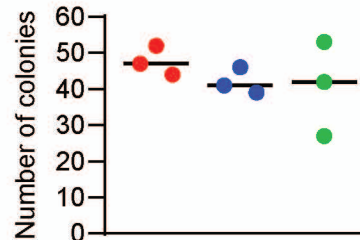
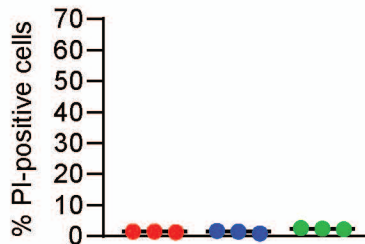
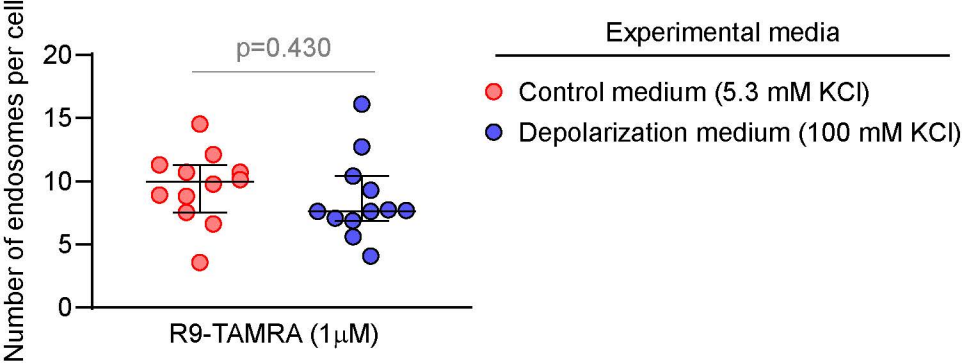


Figure S2



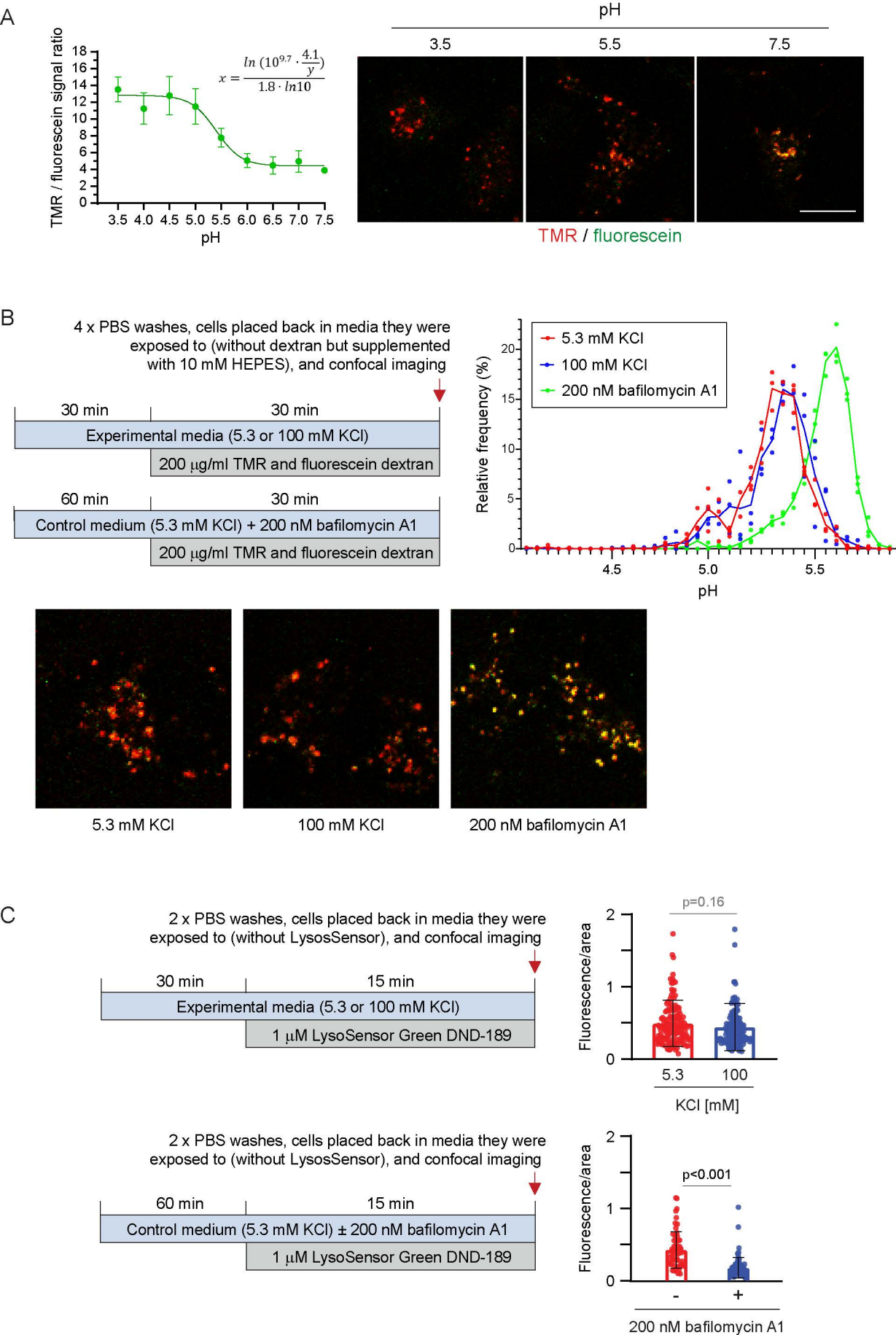


Figure S4

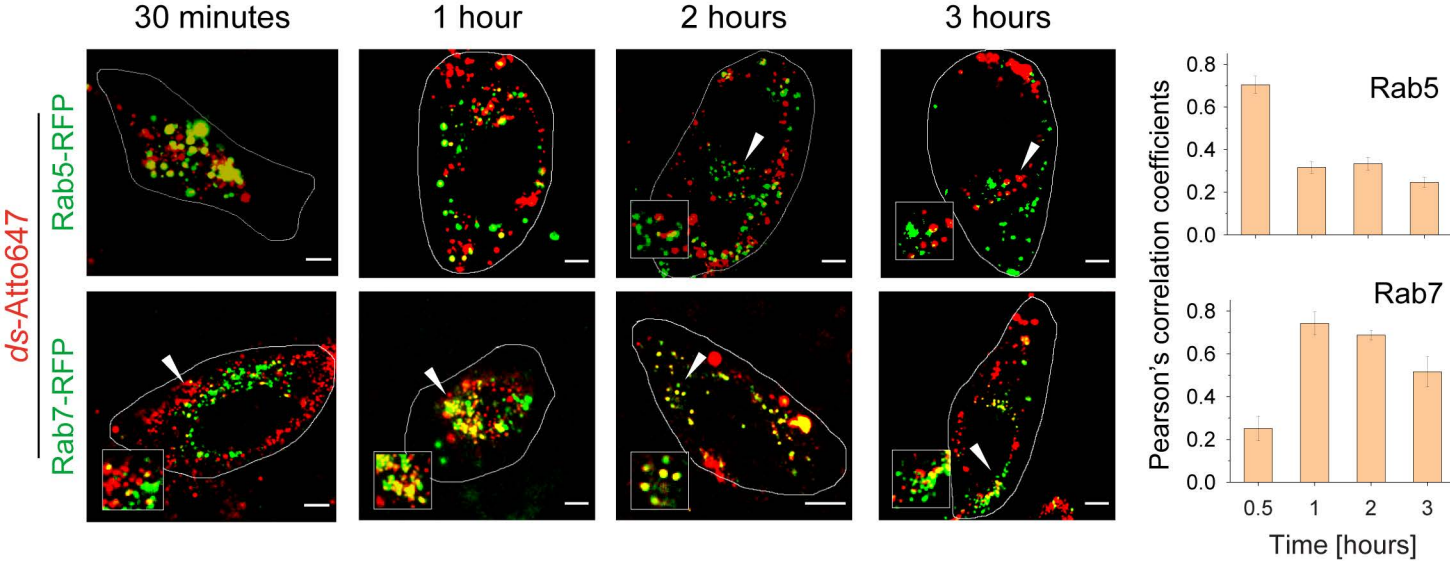


Figure S5

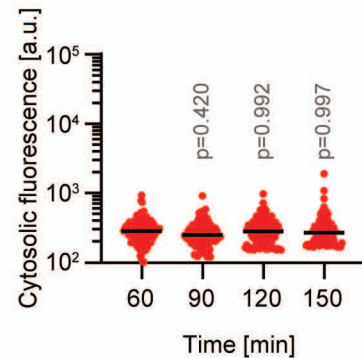
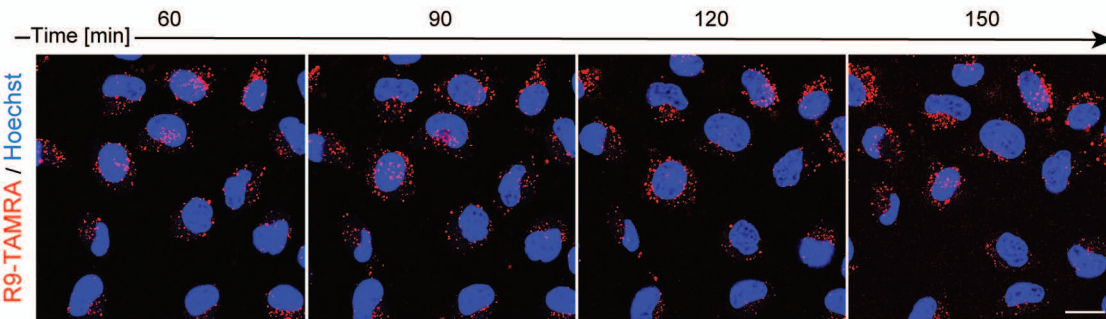
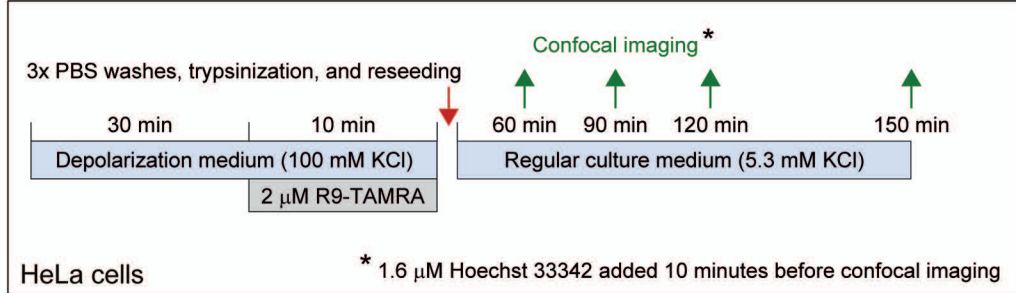


Figure S6

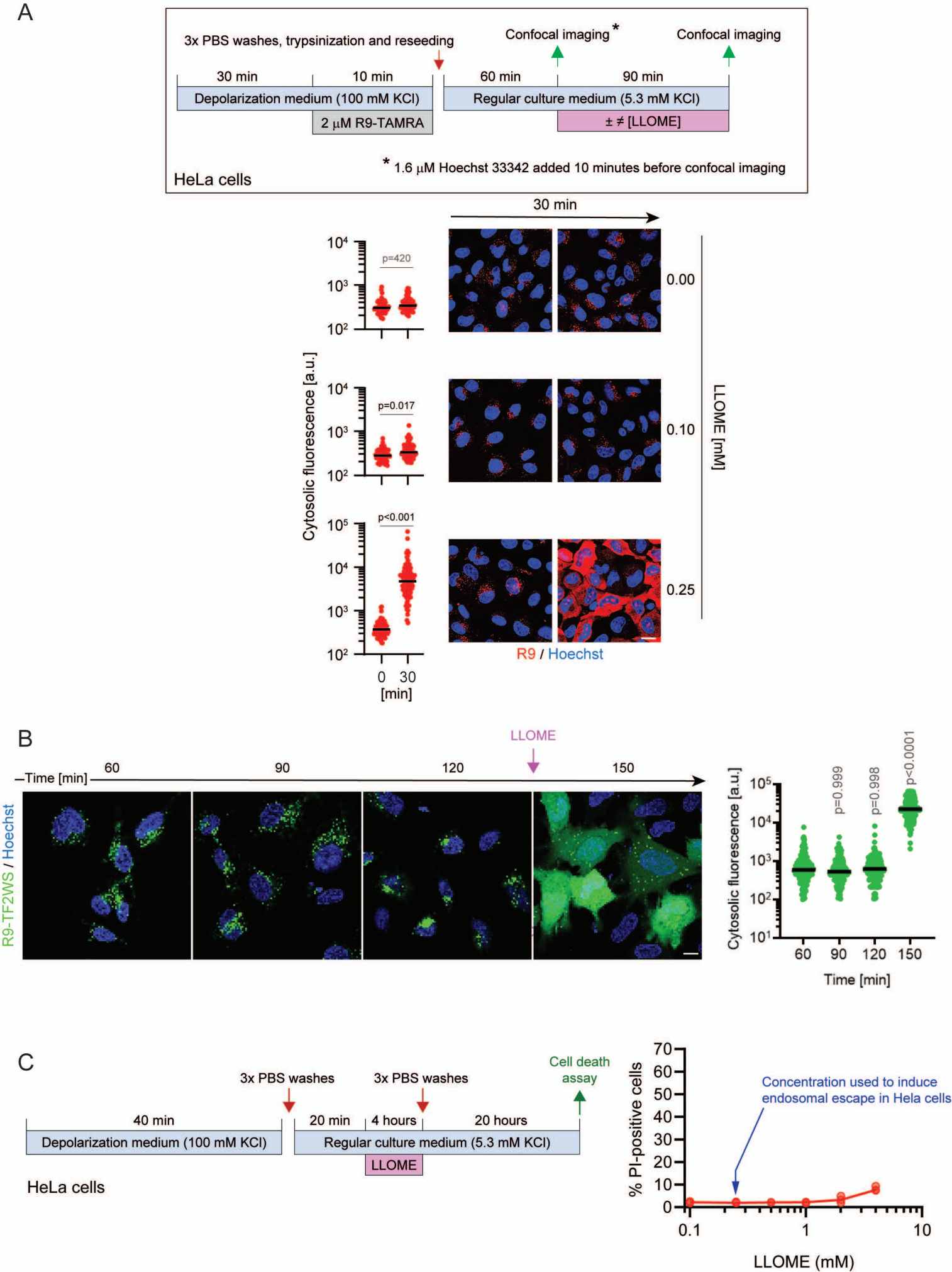


Figure S7

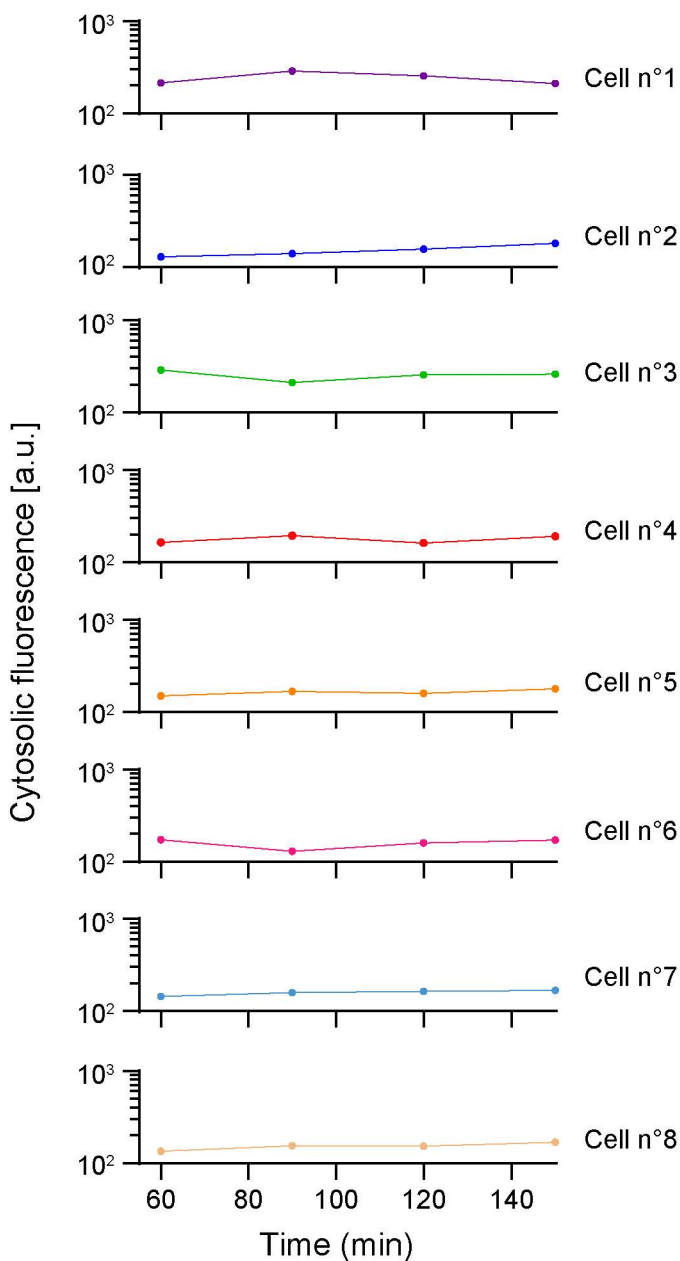
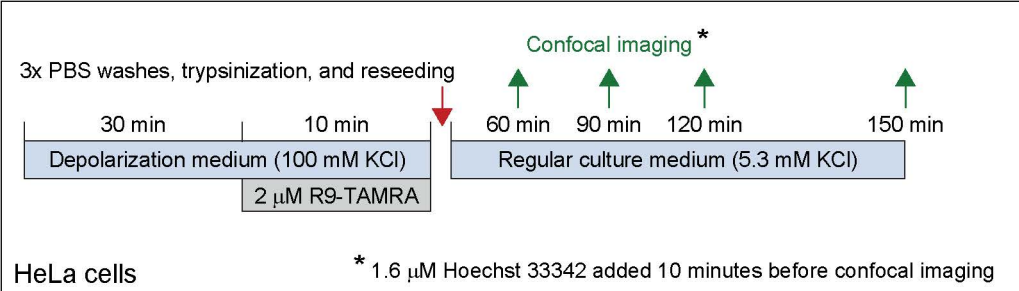


Figure S8

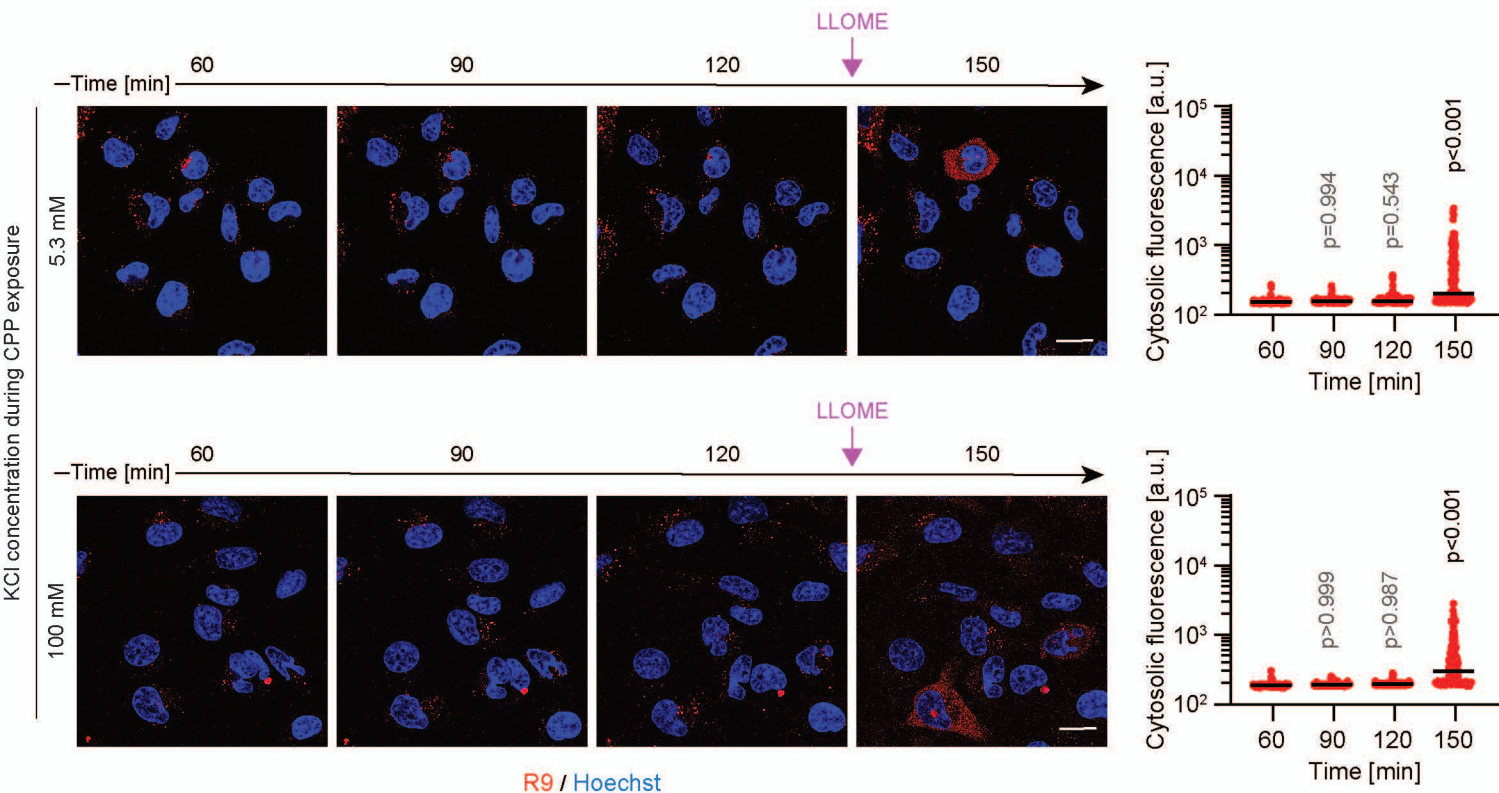
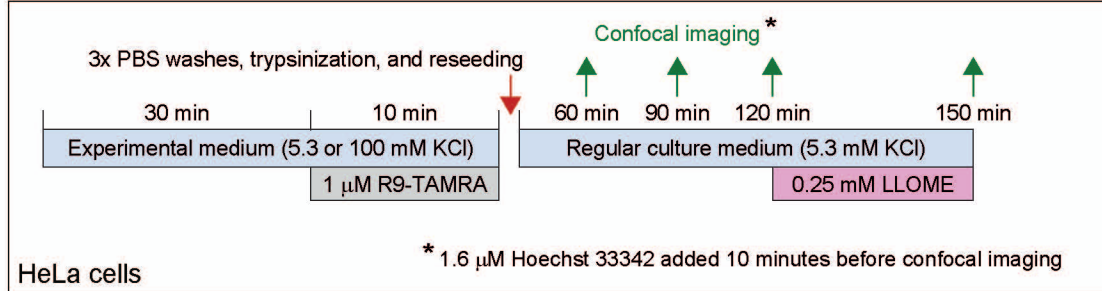


Figure S9

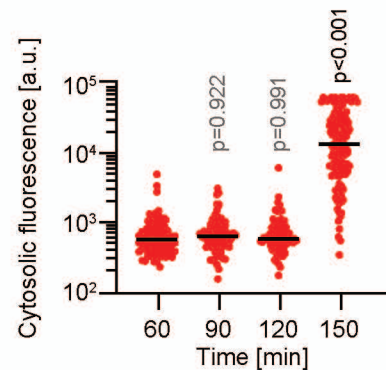
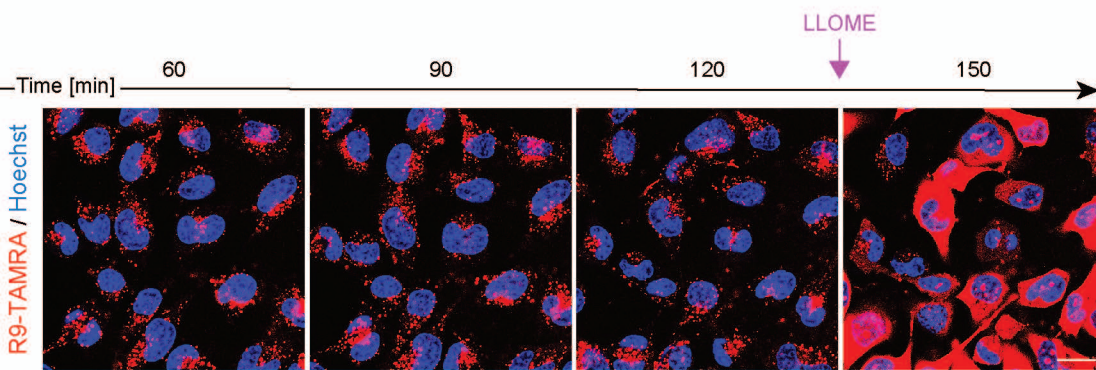
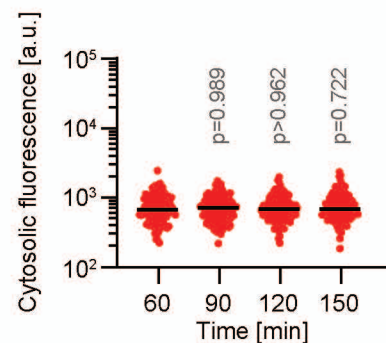
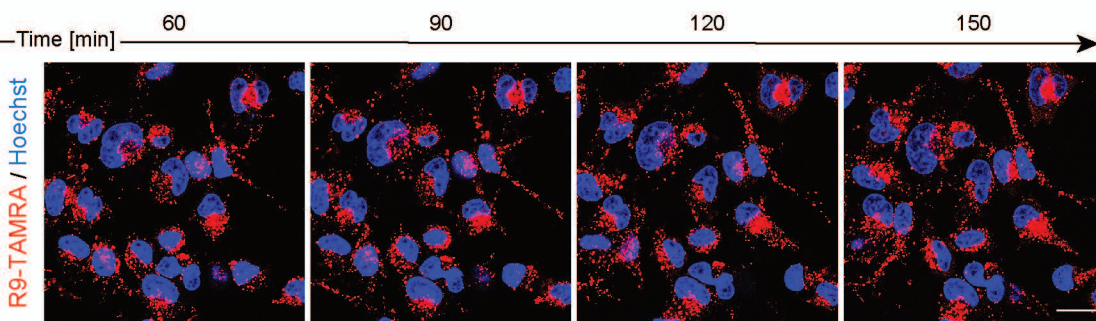
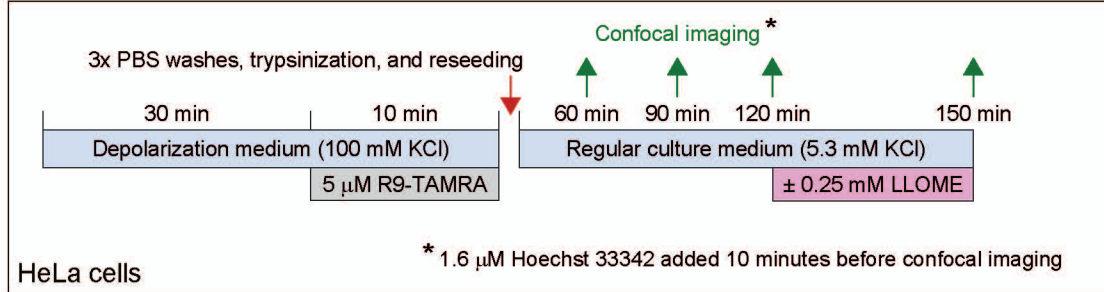
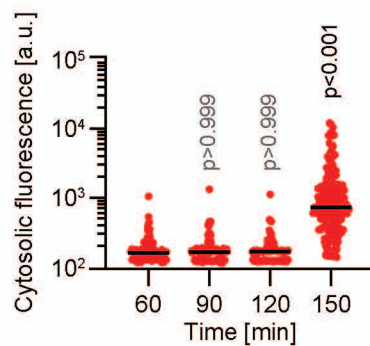
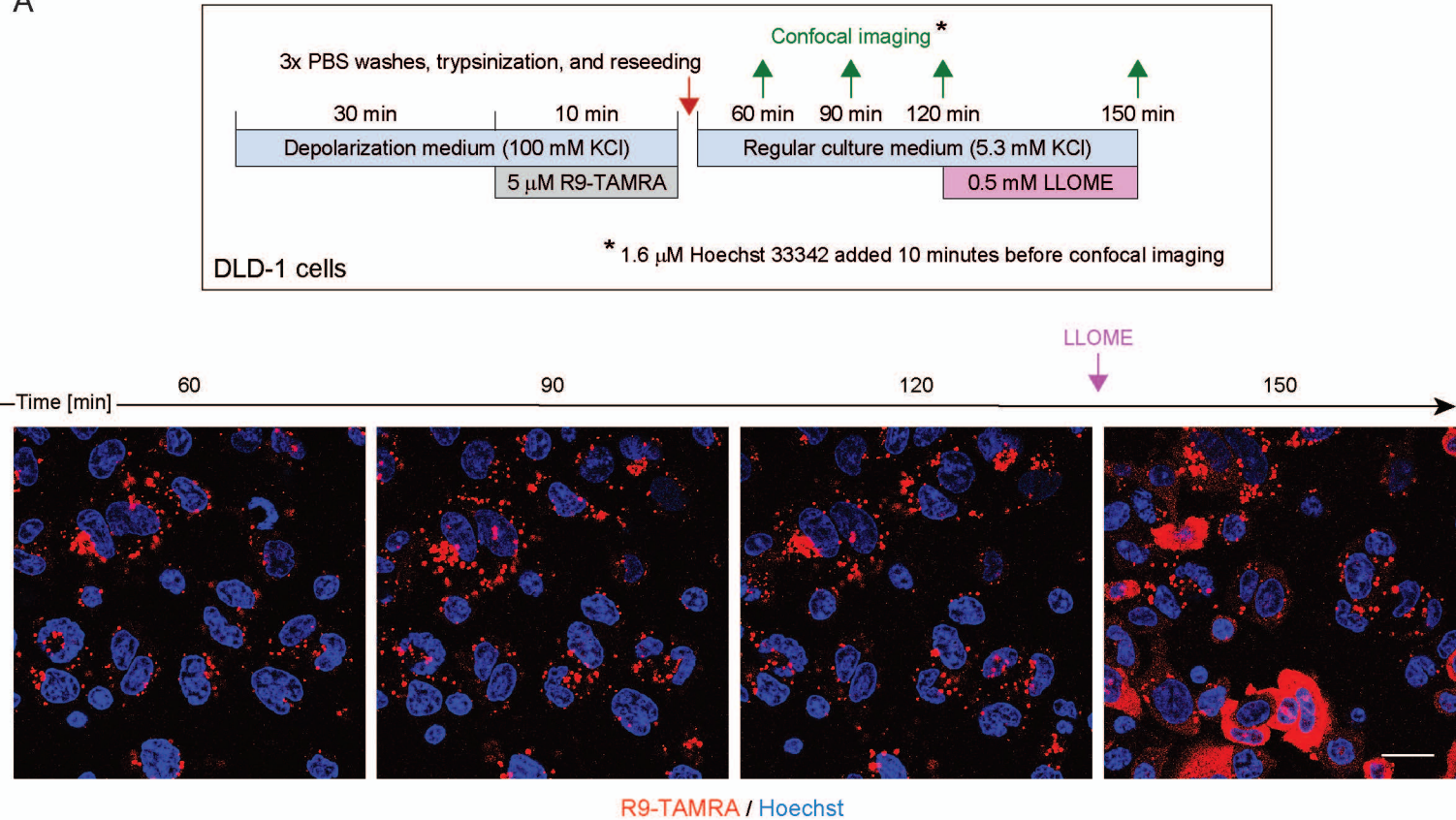


Figure S10

A



B

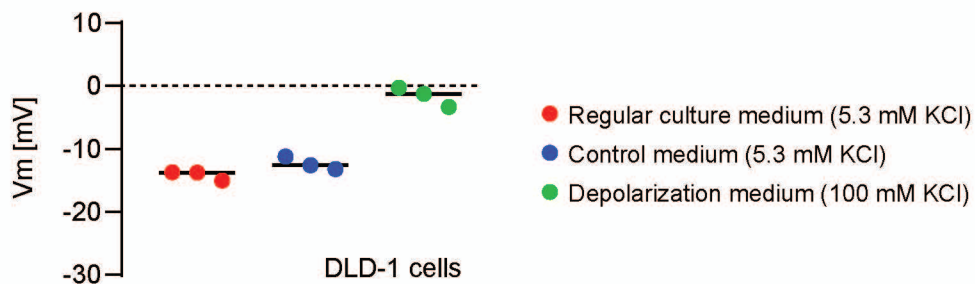
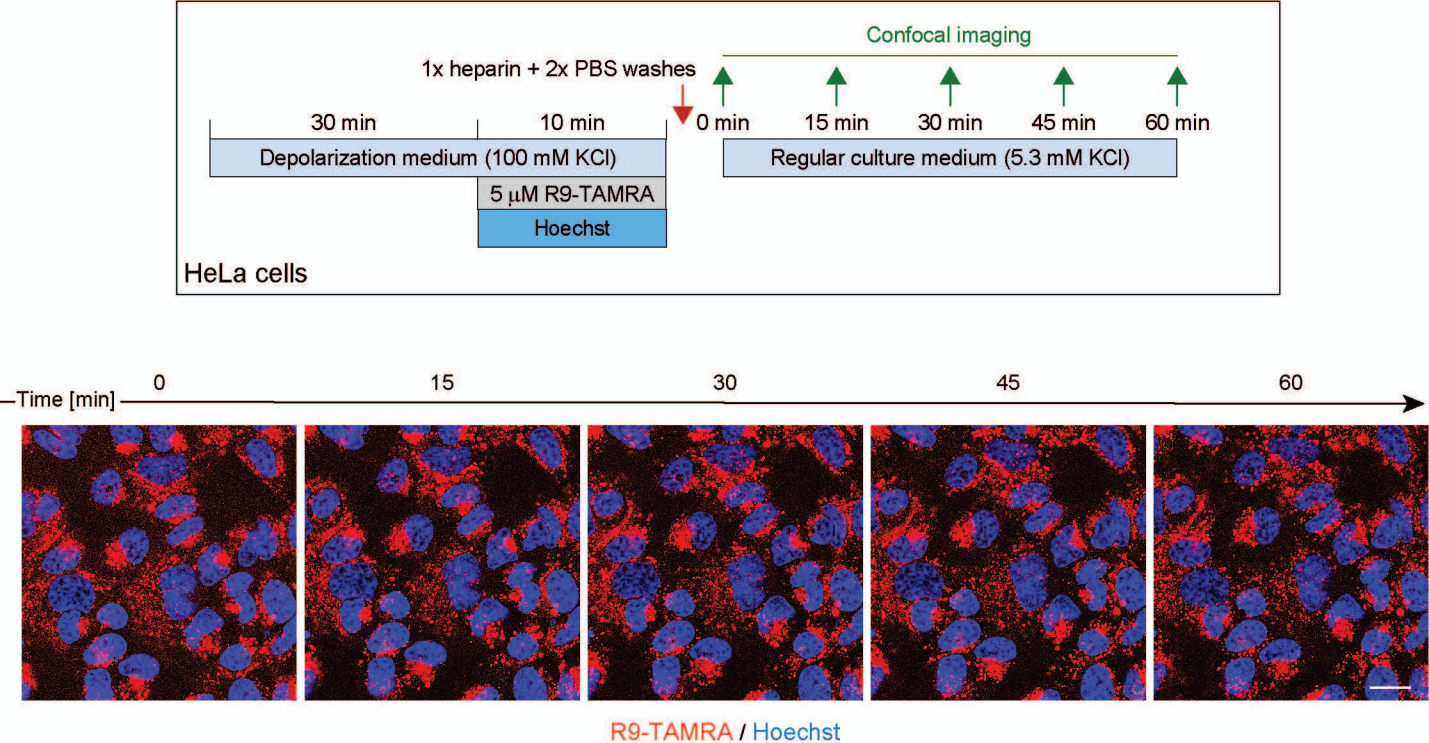


Figure S11



R9-TAMRA / Hoechst

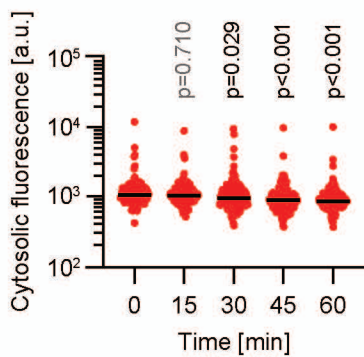


Figure S12

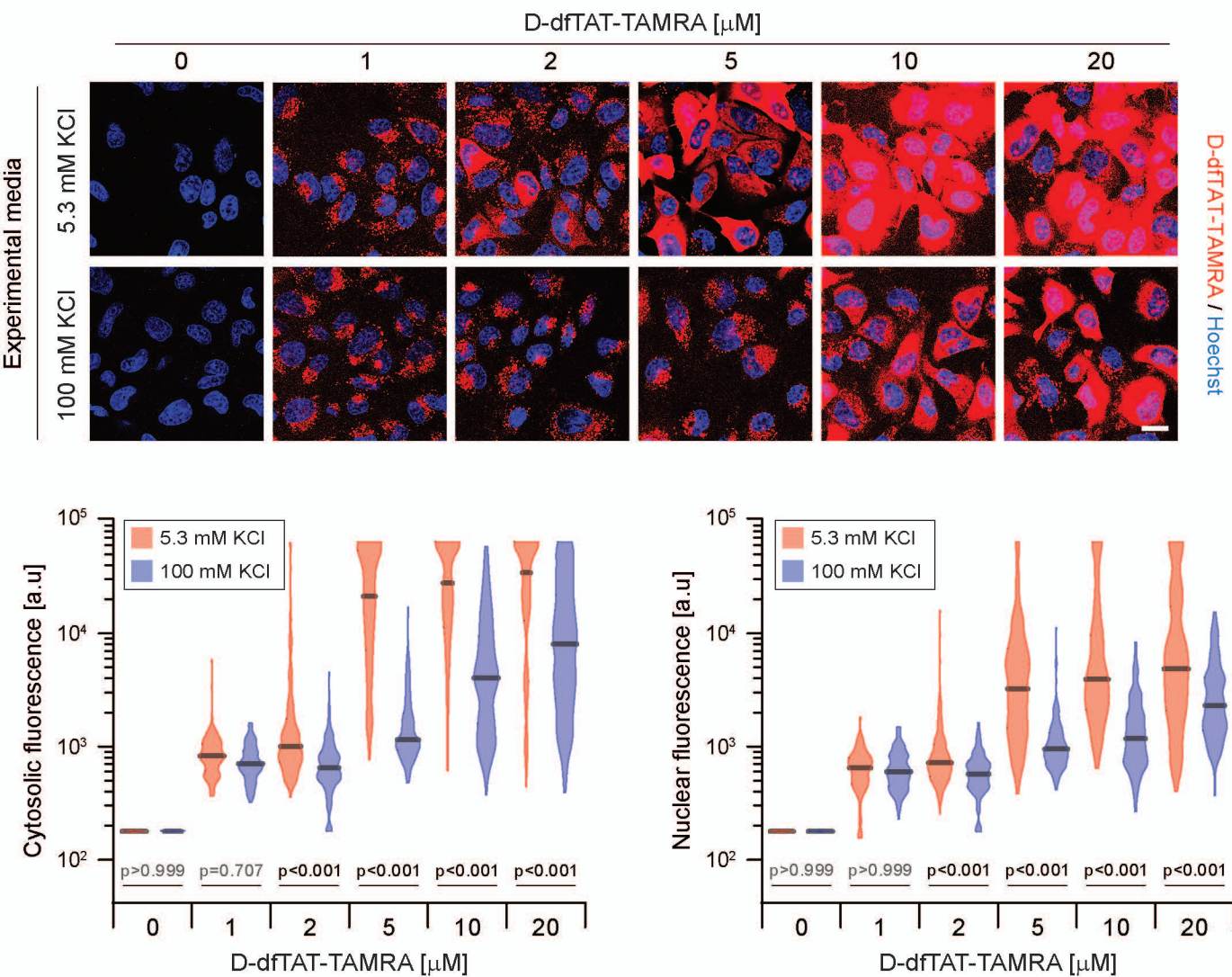
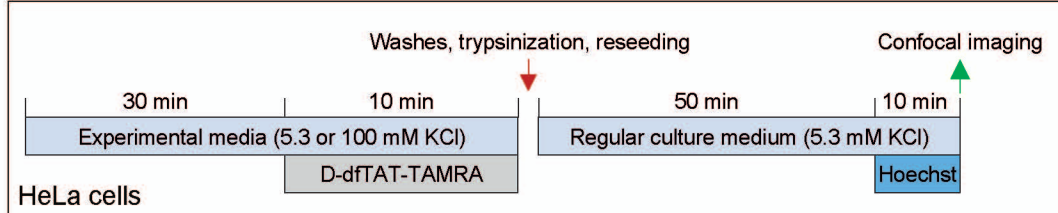


Figure S13

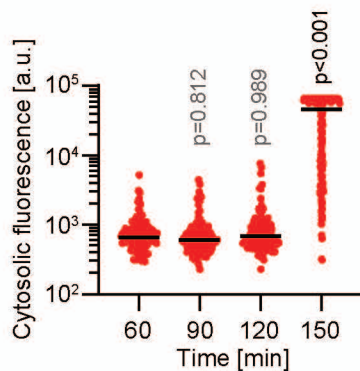
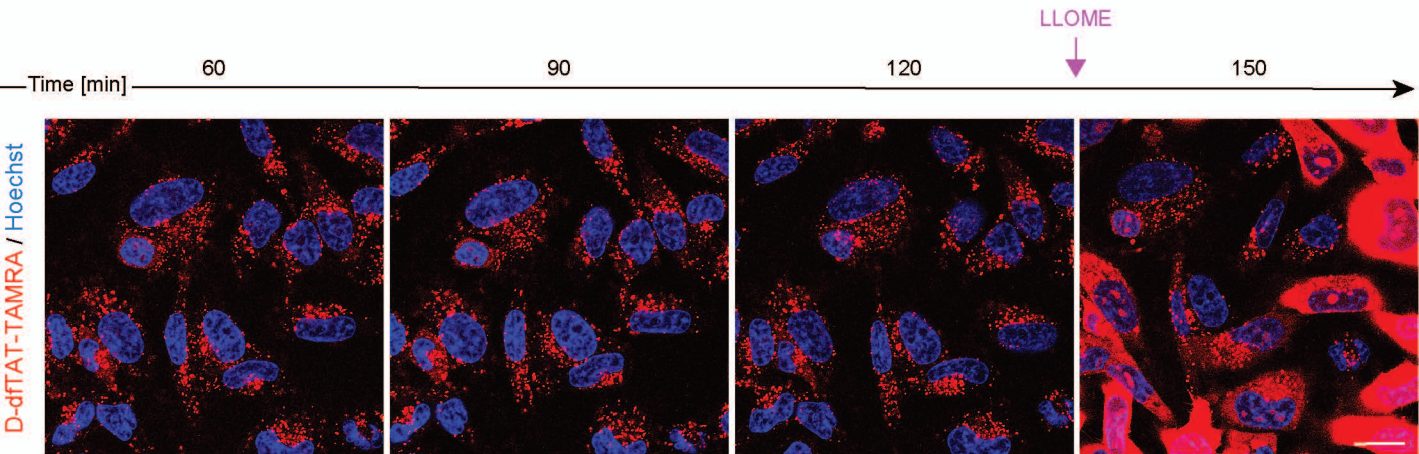
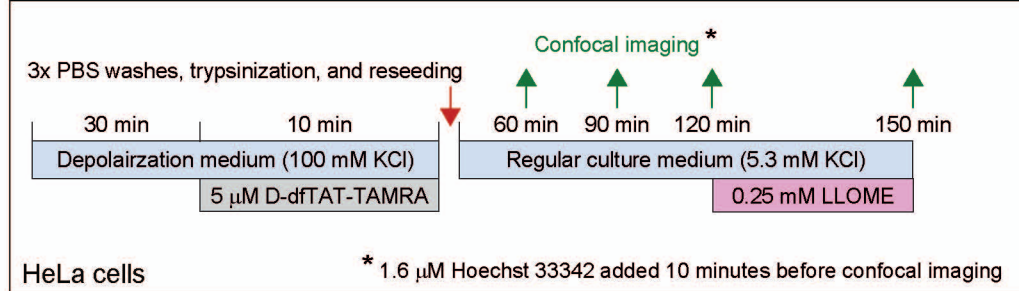


Figure S14

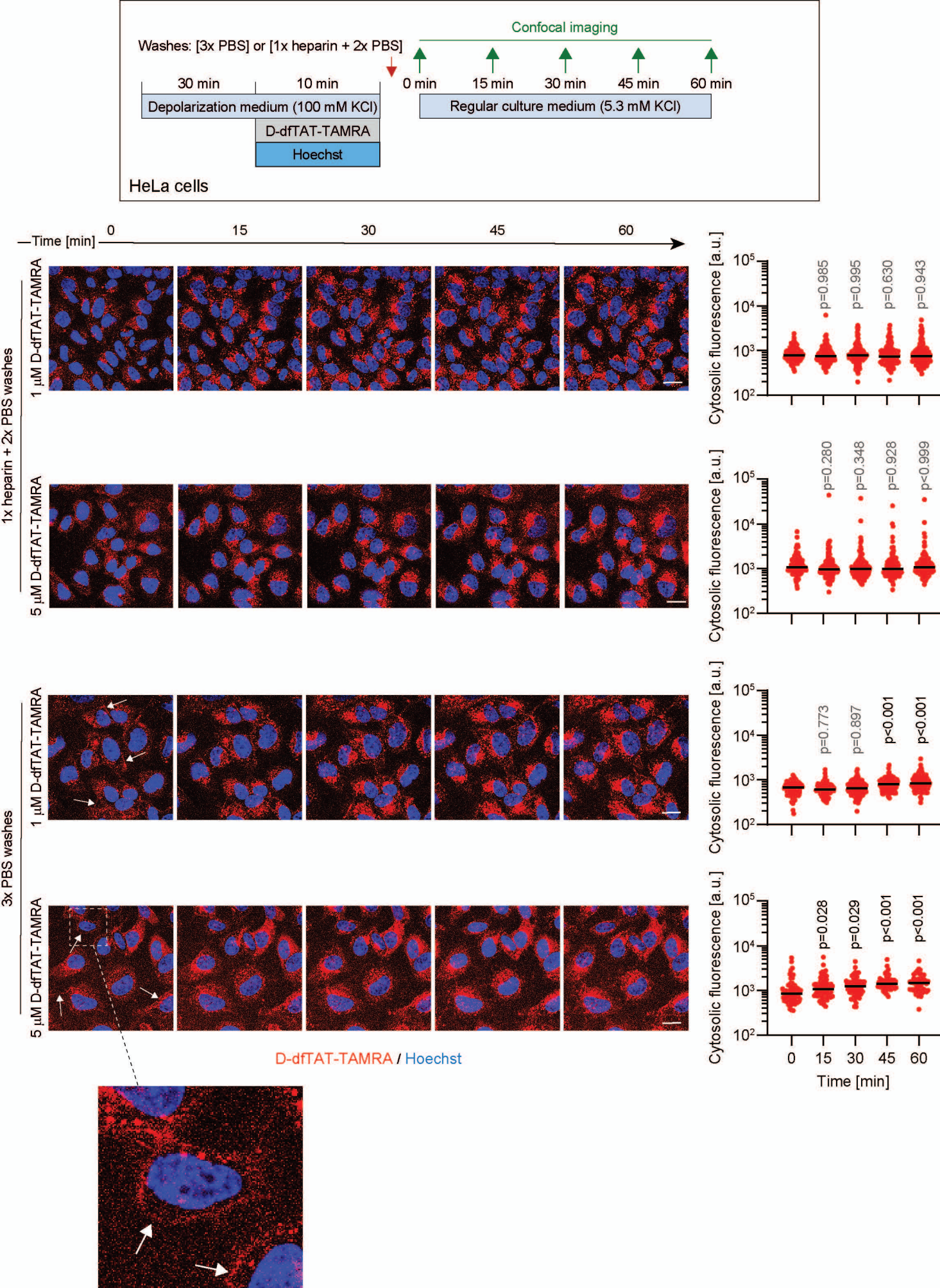


Figure S15

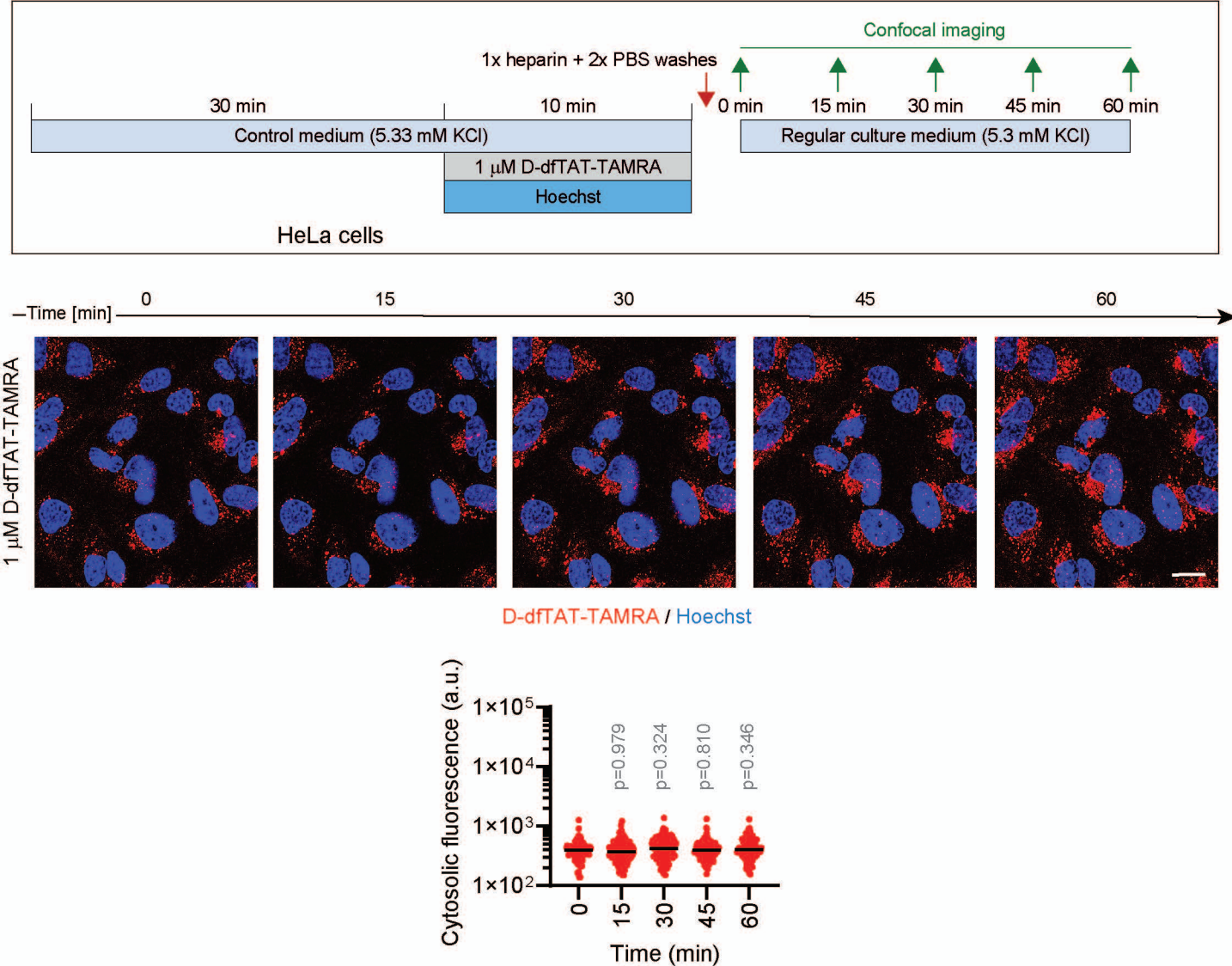


Figure S16

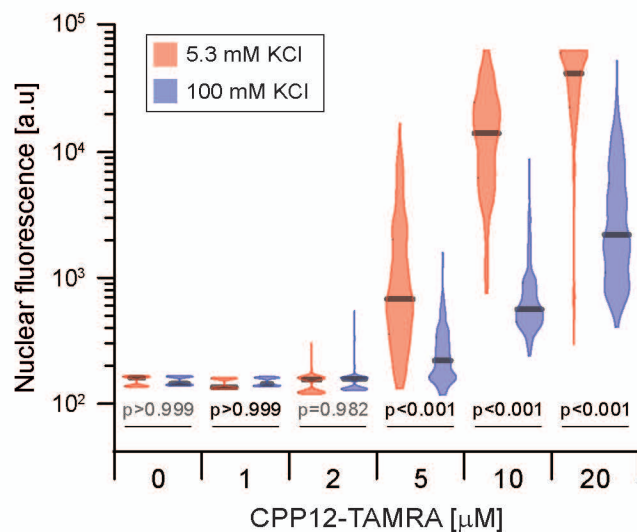
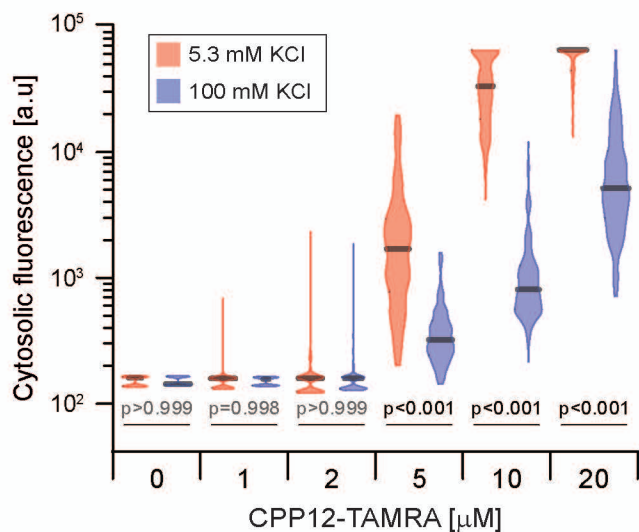
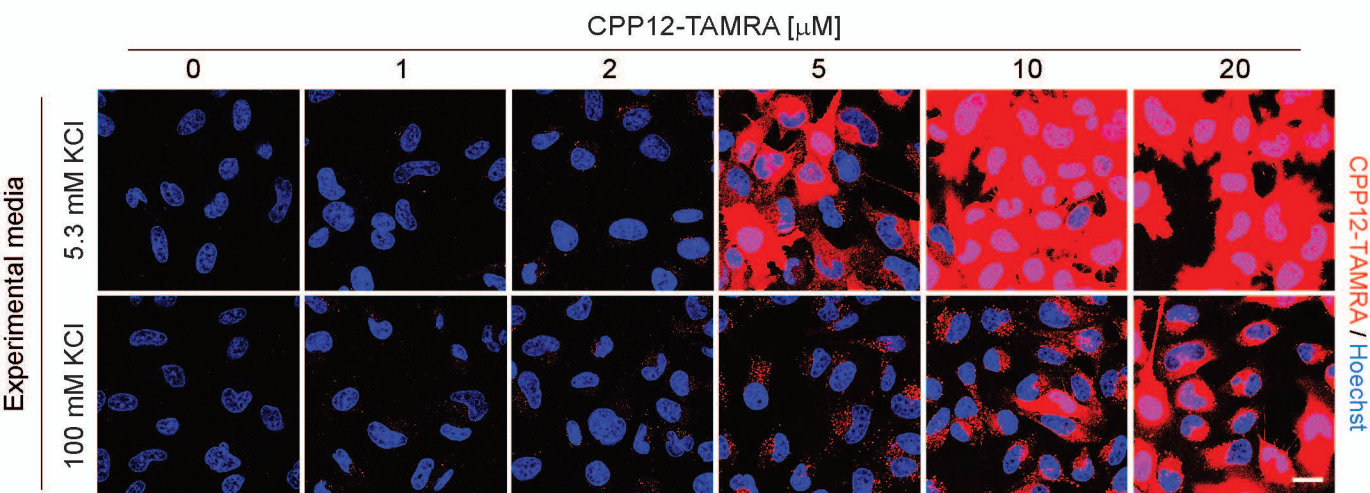
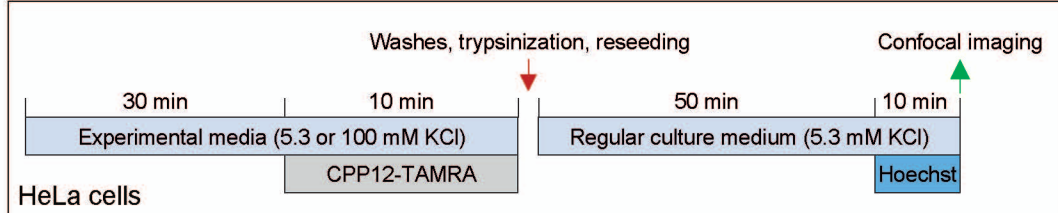
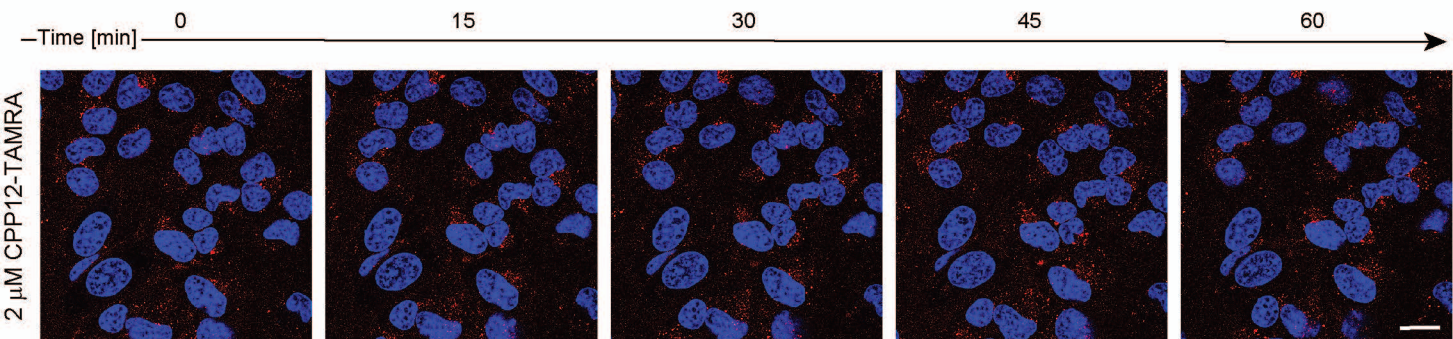
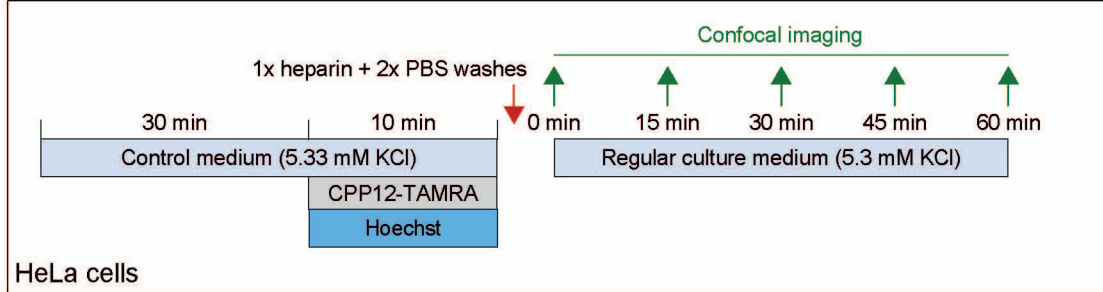


Figure S17



CPP12-TAMRA / Hoechst

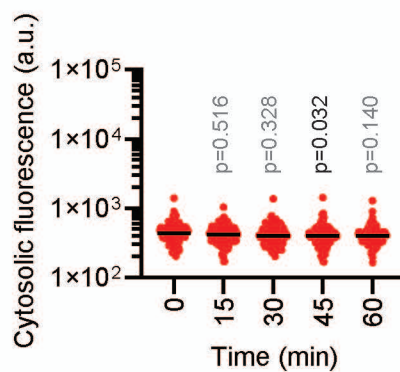


Figure S18

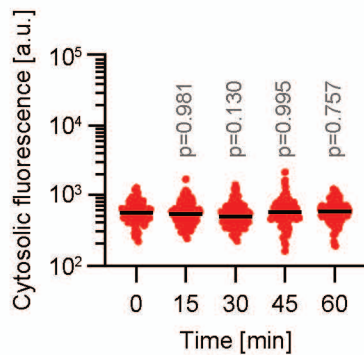
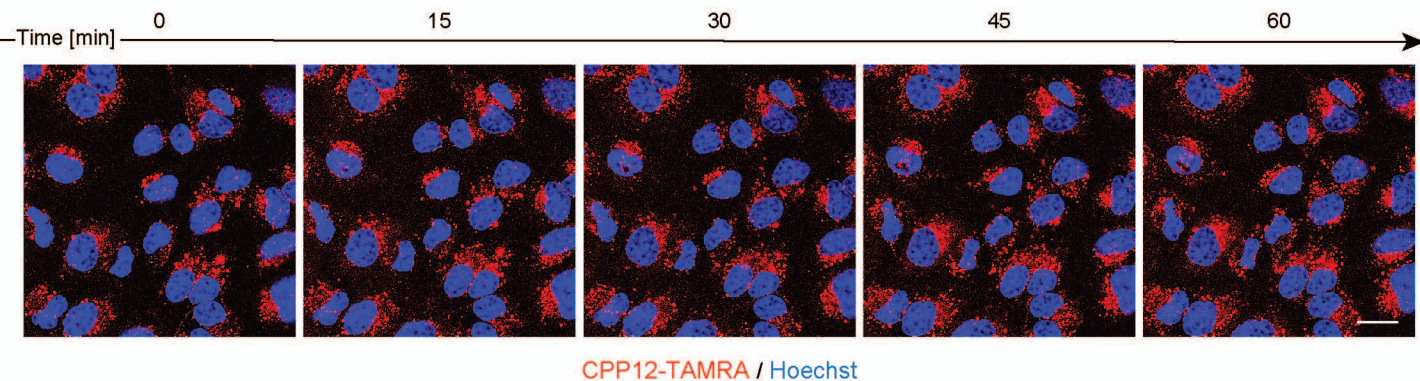
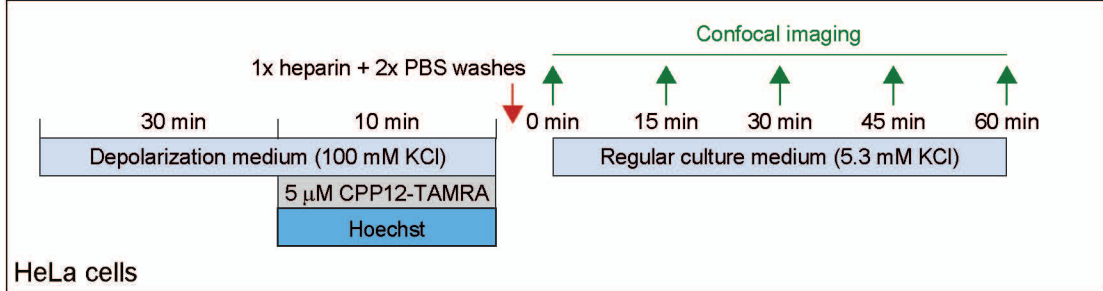


Figure S19

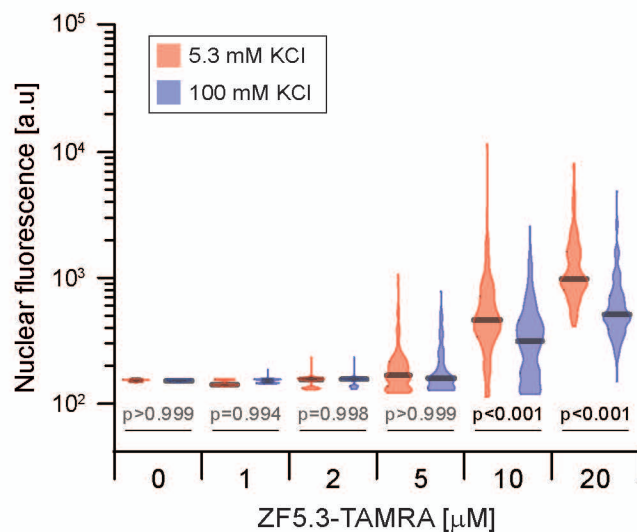
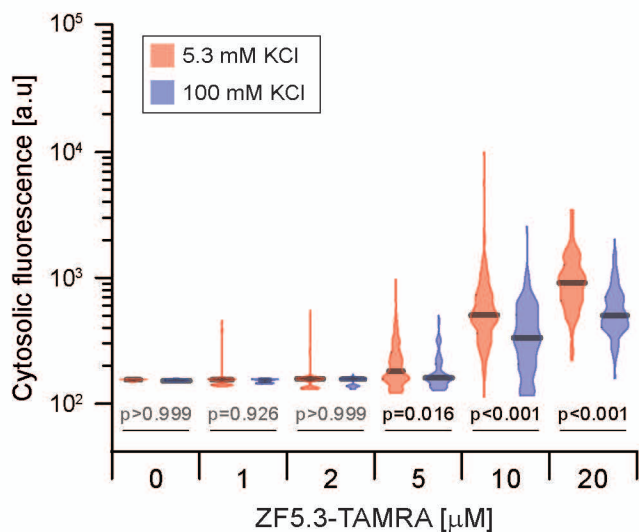
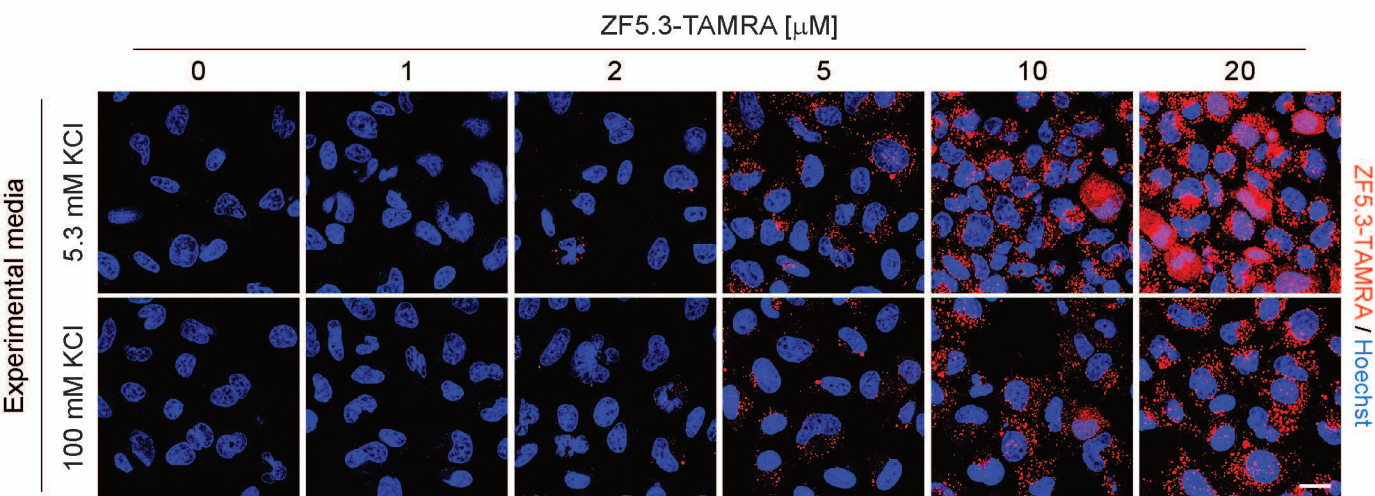
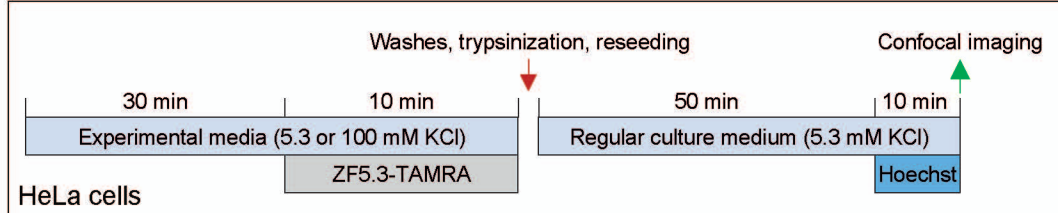


Figure S20

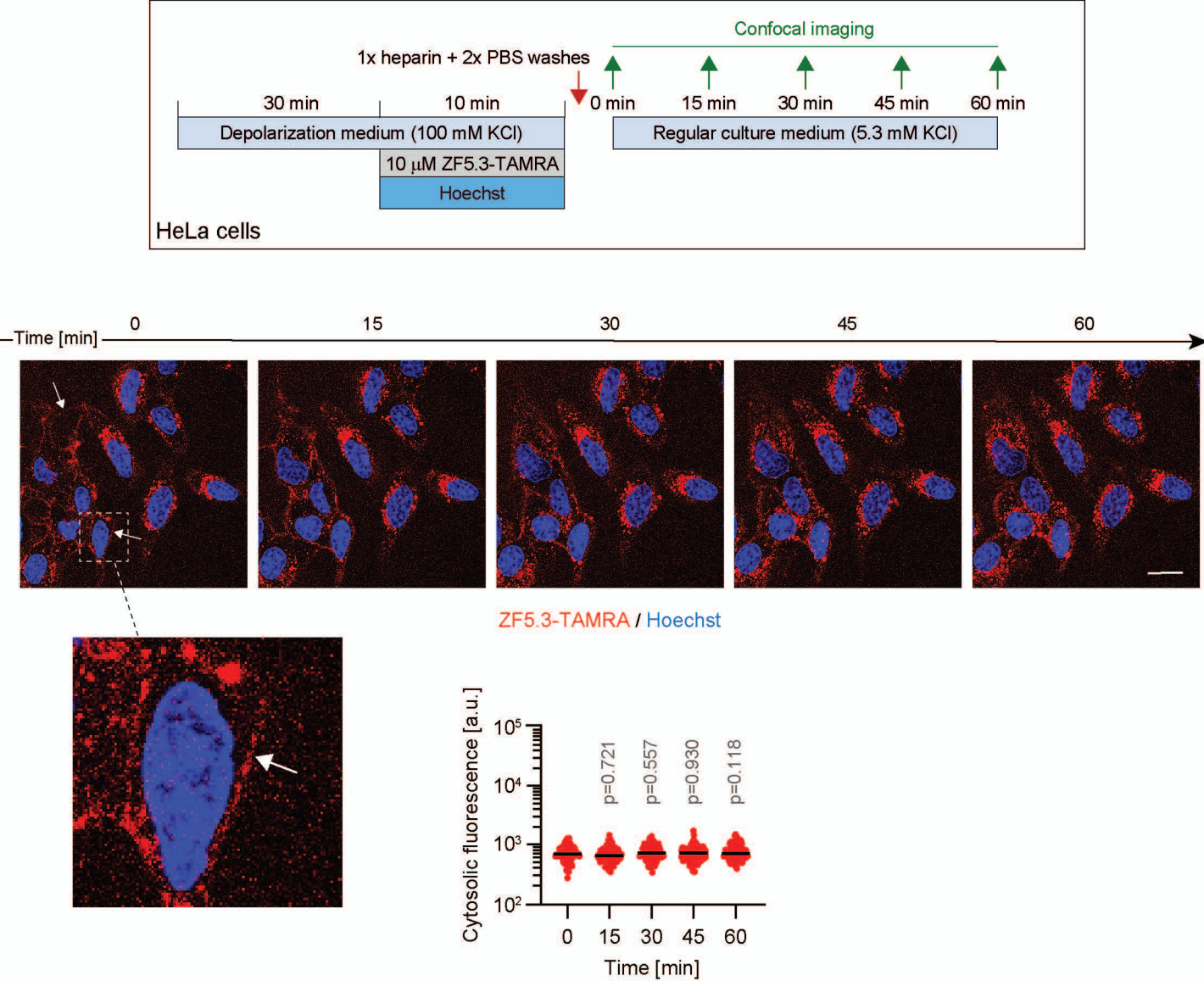


Figure S21

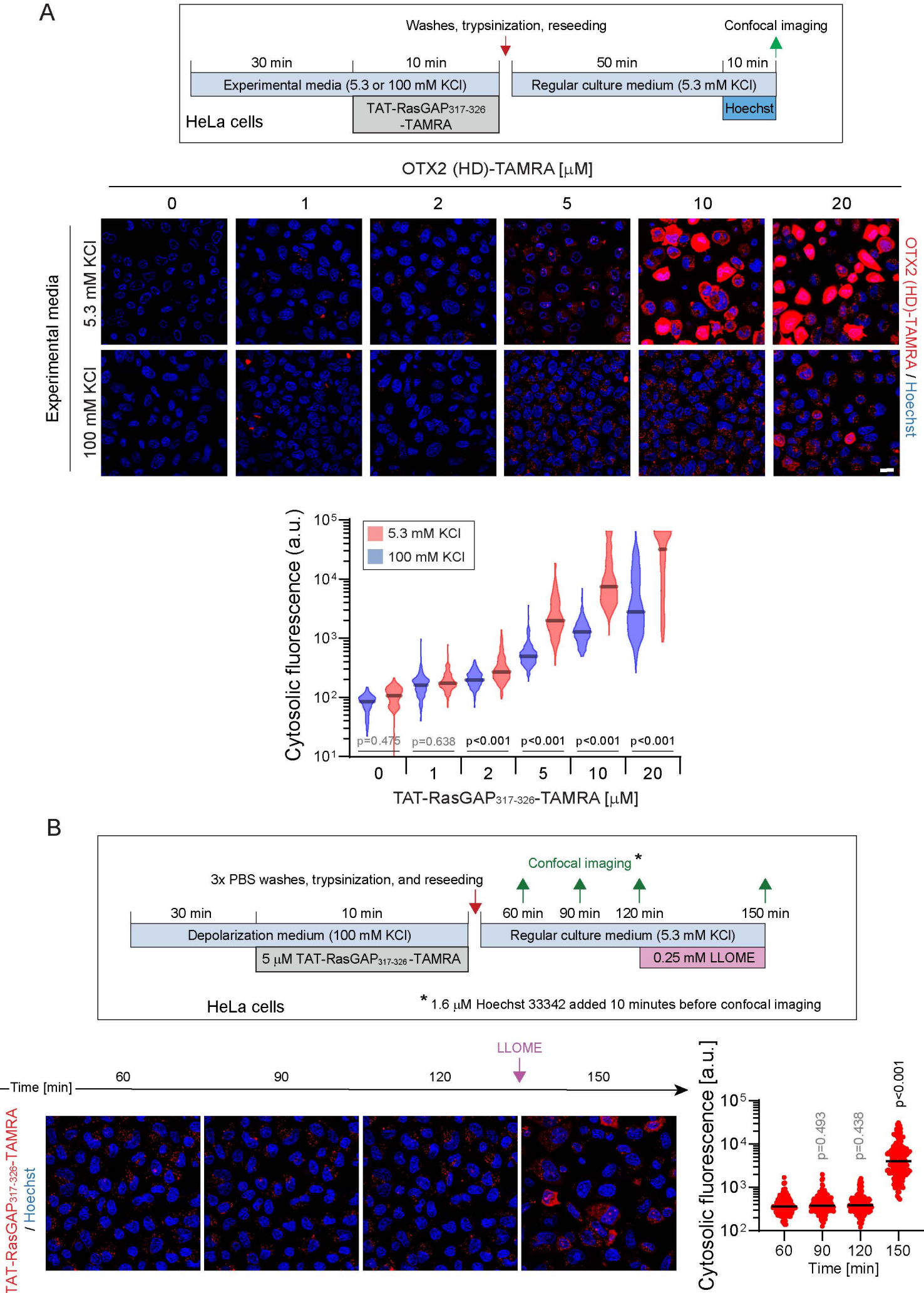
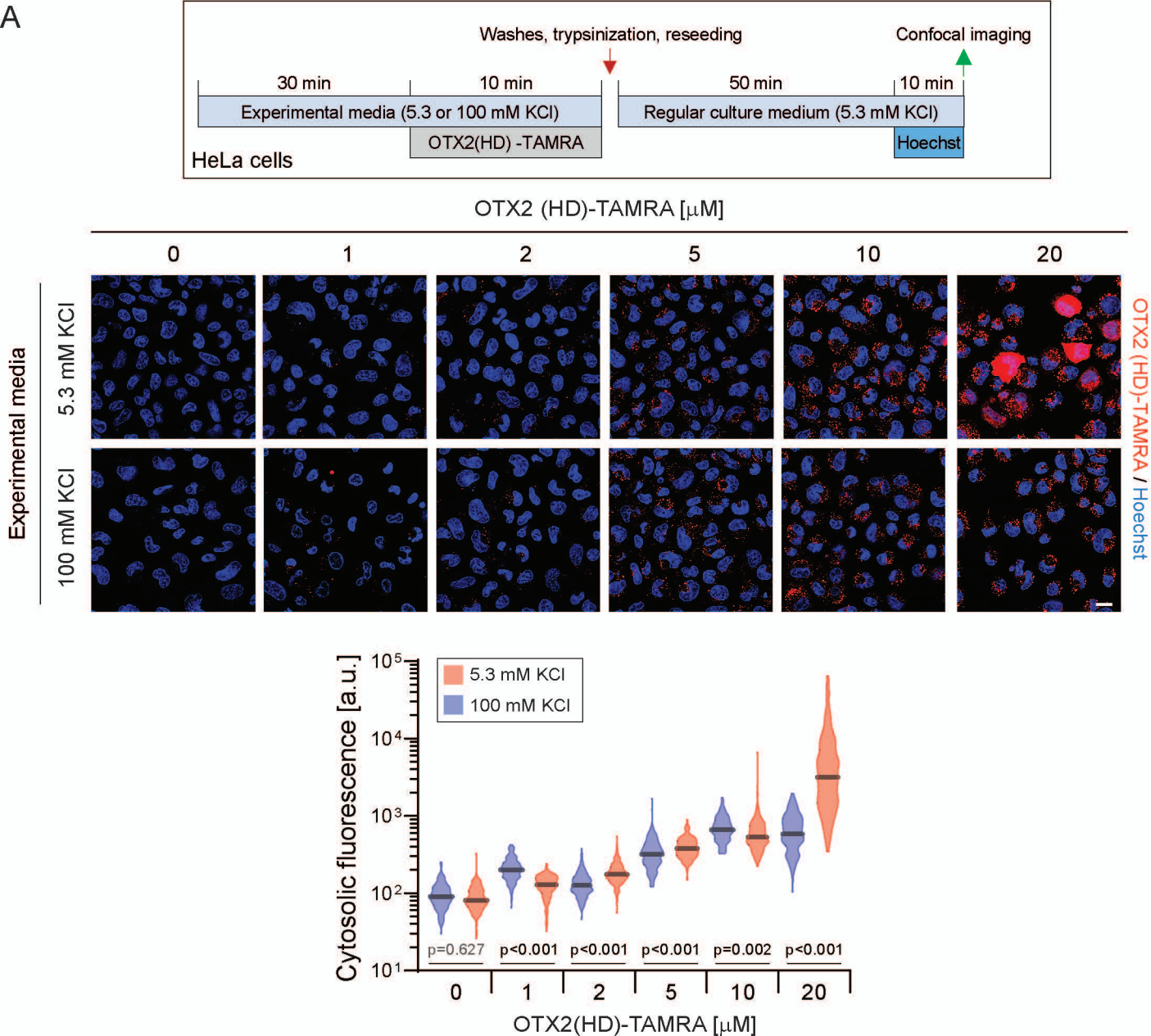


Figure S22

A



B

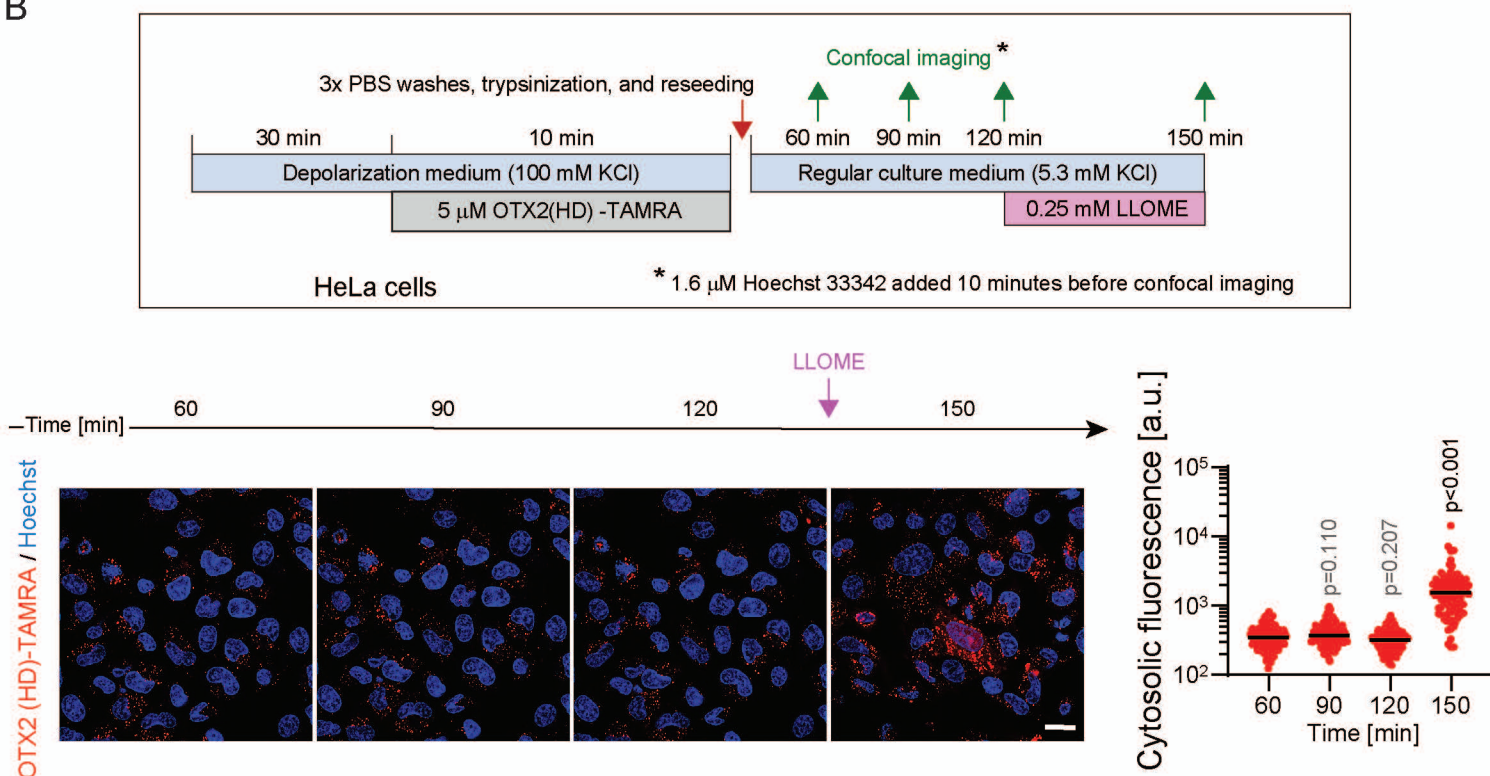
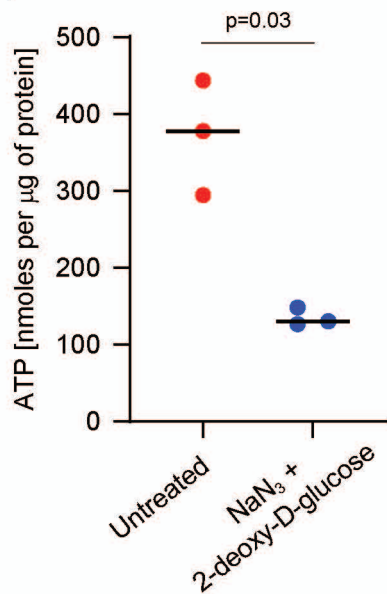
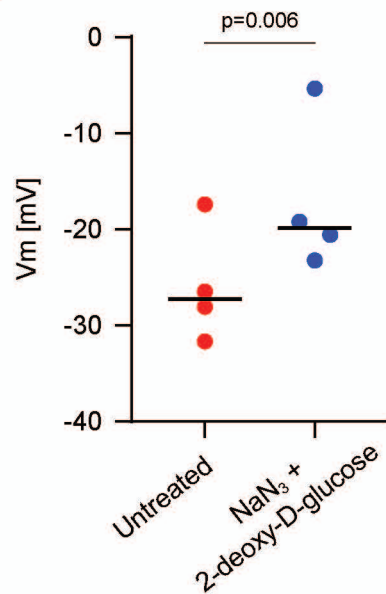


Figure S23

A



B



C

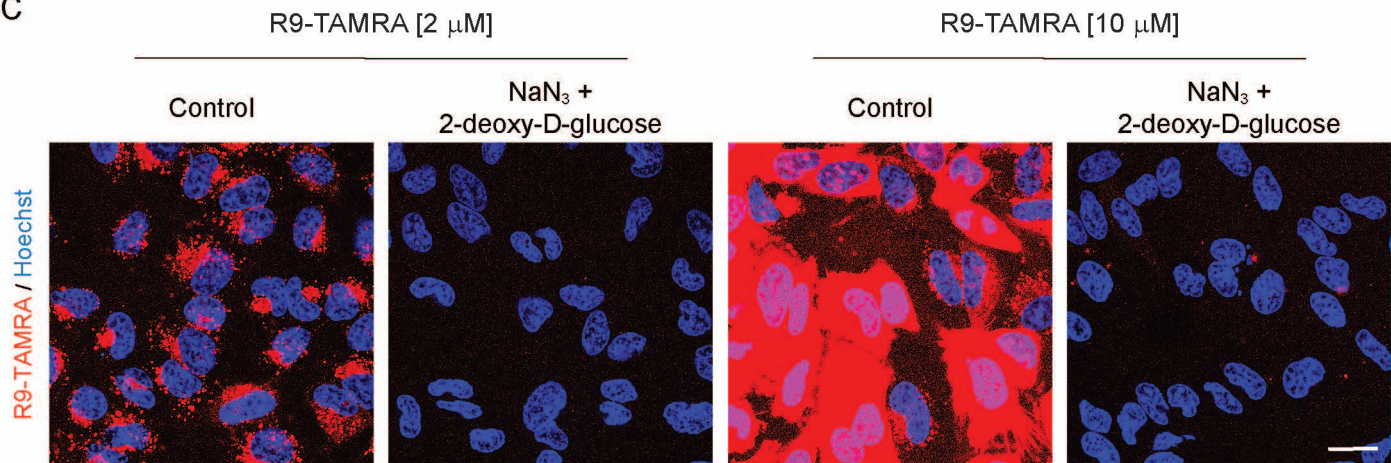
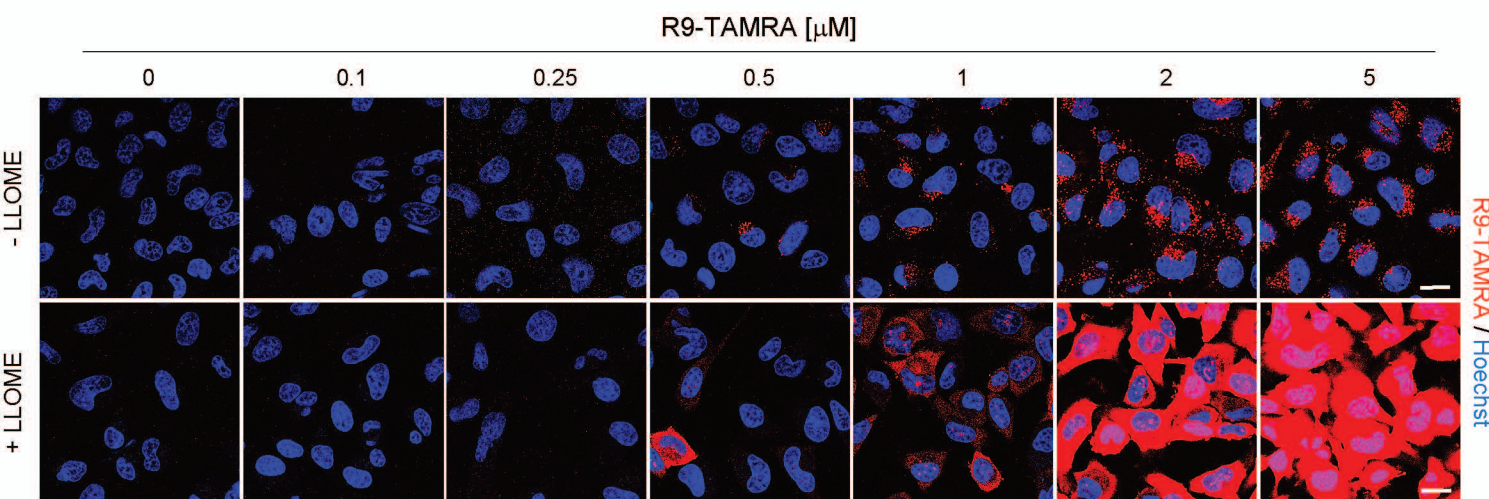
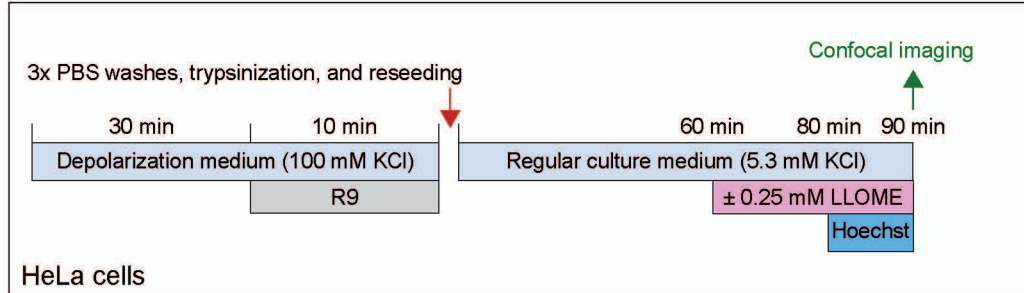
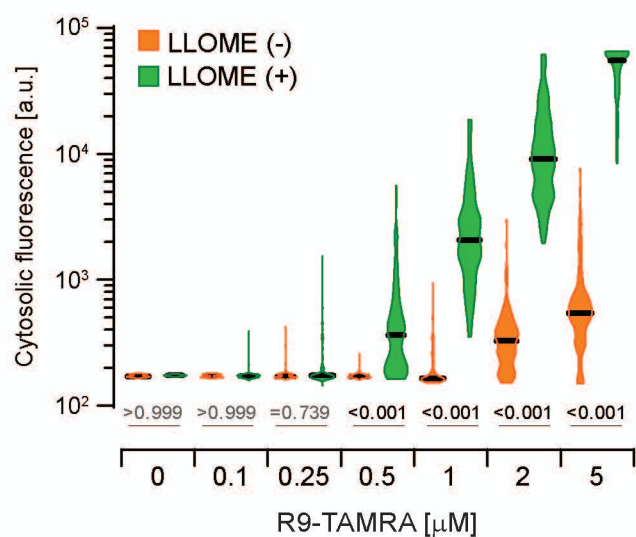


Figure S24

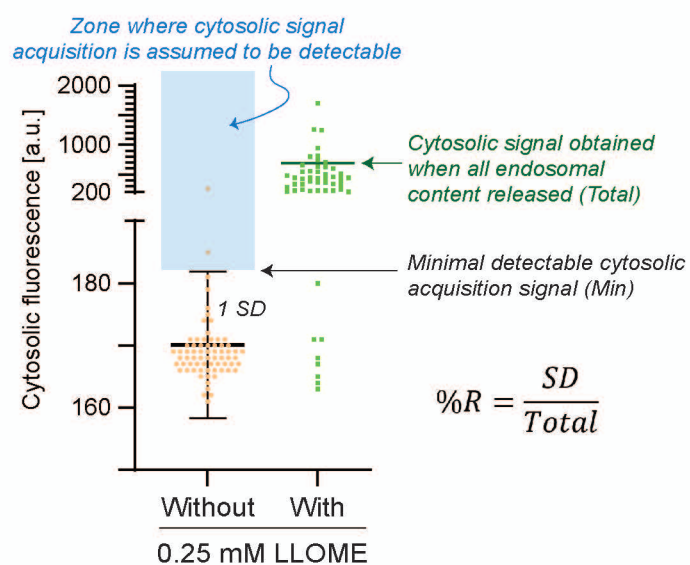
A



B



C



D

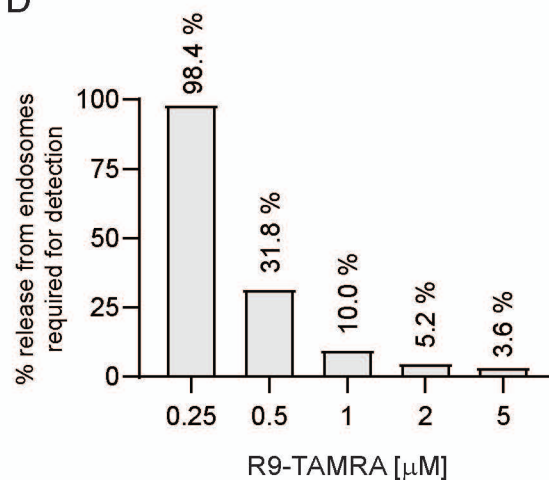


Figure S25

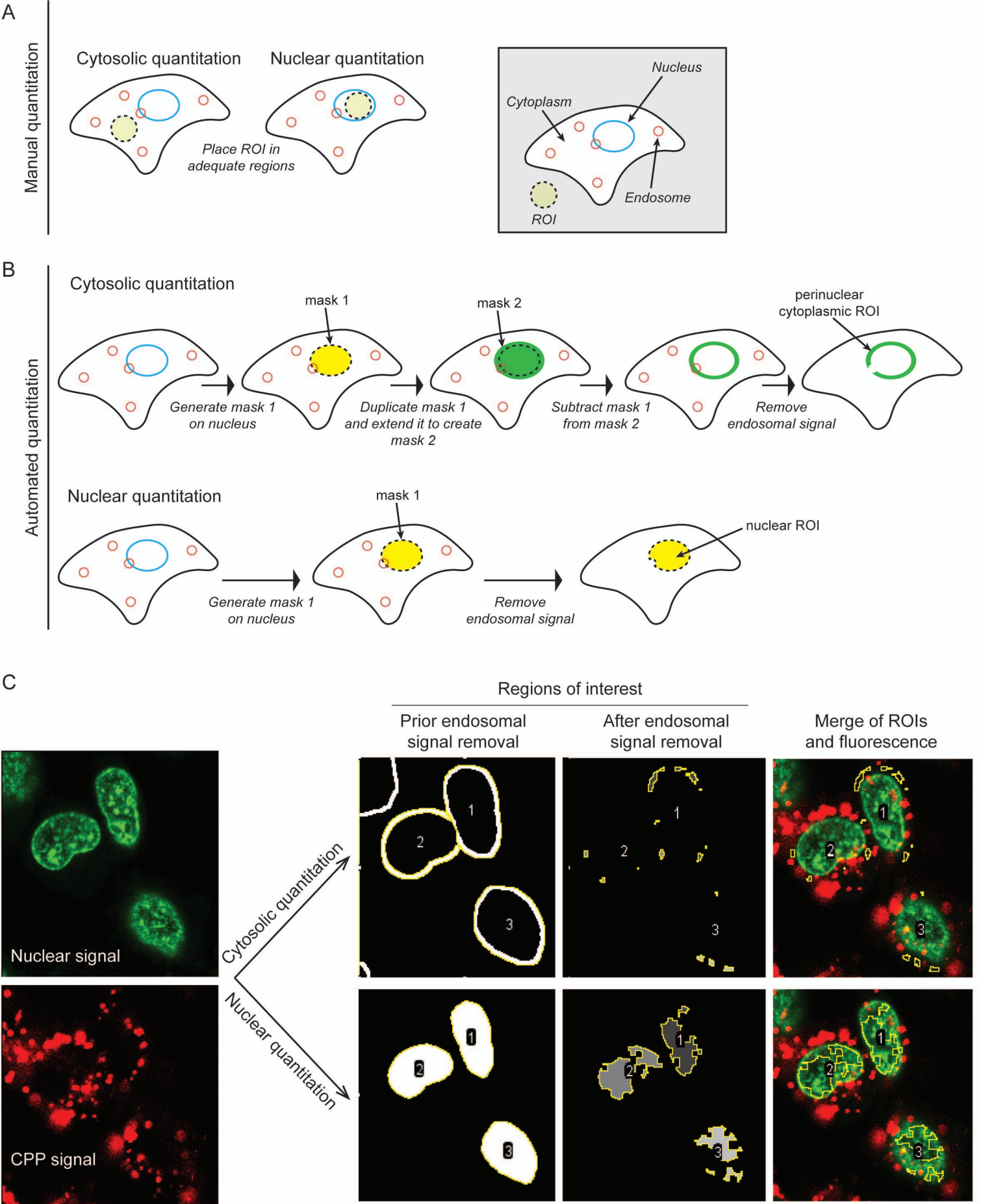
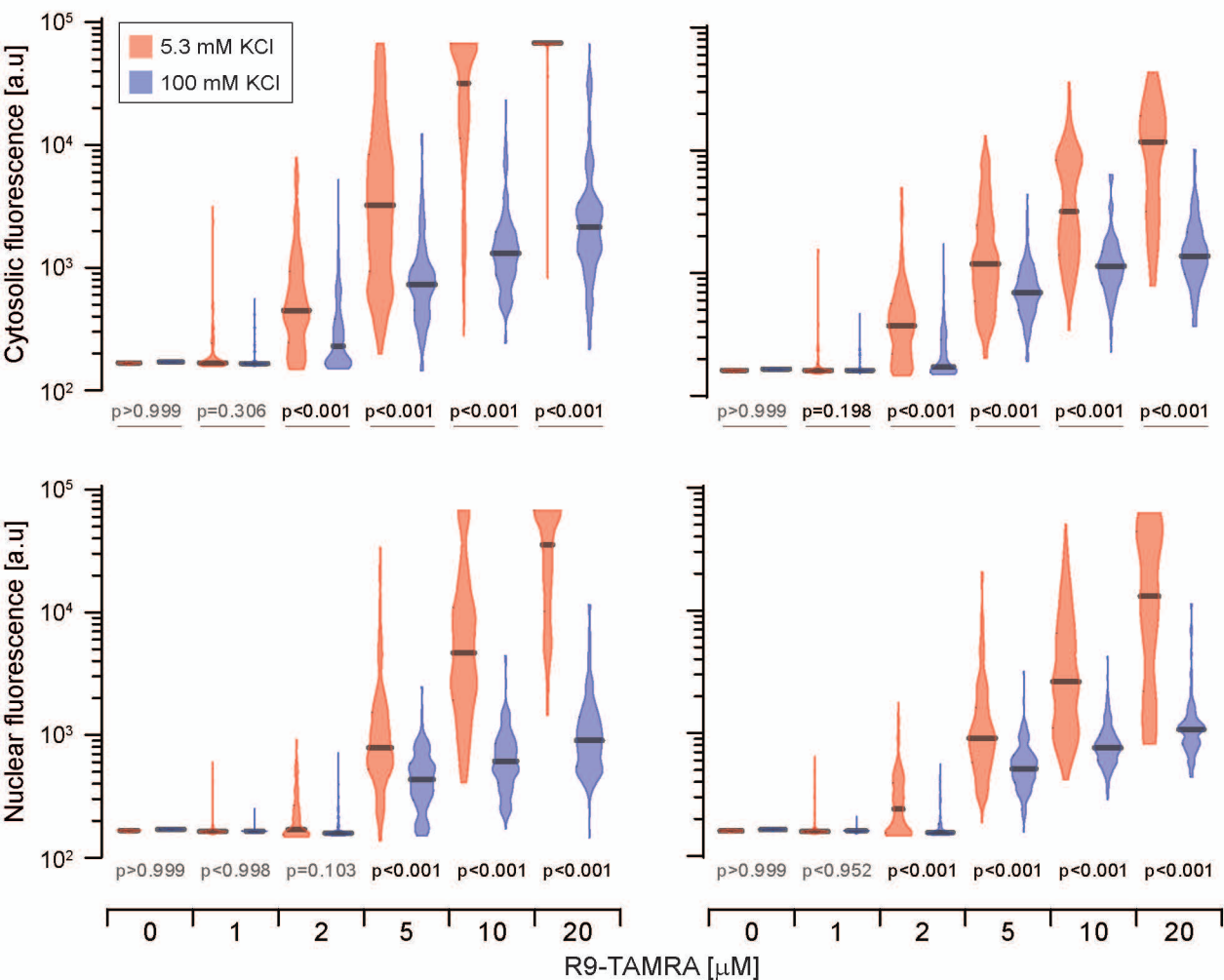


Figure S26

Manual quantitation

Automated quantitation



p values for the comparison with the "0 μM R9-TAMRA" condition

		Manual					Automated				
	mM KCl	1	2	5	10	20	1	2	5	10	20
Cytosol	5.3	0.196	<0.001	<0.001	<0.001	<0.001	0.04	<0.001	<0.001	<0.001	<0.001
	100	>0.999	0.002	<0.001	<0.001	<0.001	0.999	<0.001	<0.001	<0.001	<0.001
Nucleus	5.3	0.998	0.041	<0.001	<0.001	<0.001	0.884	<0.001	<0.001	<0.001	<0.001
	100	0.997	0.996	<0.001	<0.001	<0.001	0.993	0.305	<0.001	<0.001	<0.001

Figure S27